PB96-143177

REPORT NO.
UCB/EERC-95/08
AUGUST 1995

EARTHQUAKE ENGINEERING RESEARCH CENTER

BEHAVIOR OF PRE-NORTHRIDGE MOMENT RESISTING STEEL CONNECTIONS

by

TZONG-SHUOH YANG
EGOR P. POPOV

Report to Sponsors:
National Science Foundation
American Institute of Steel Construction

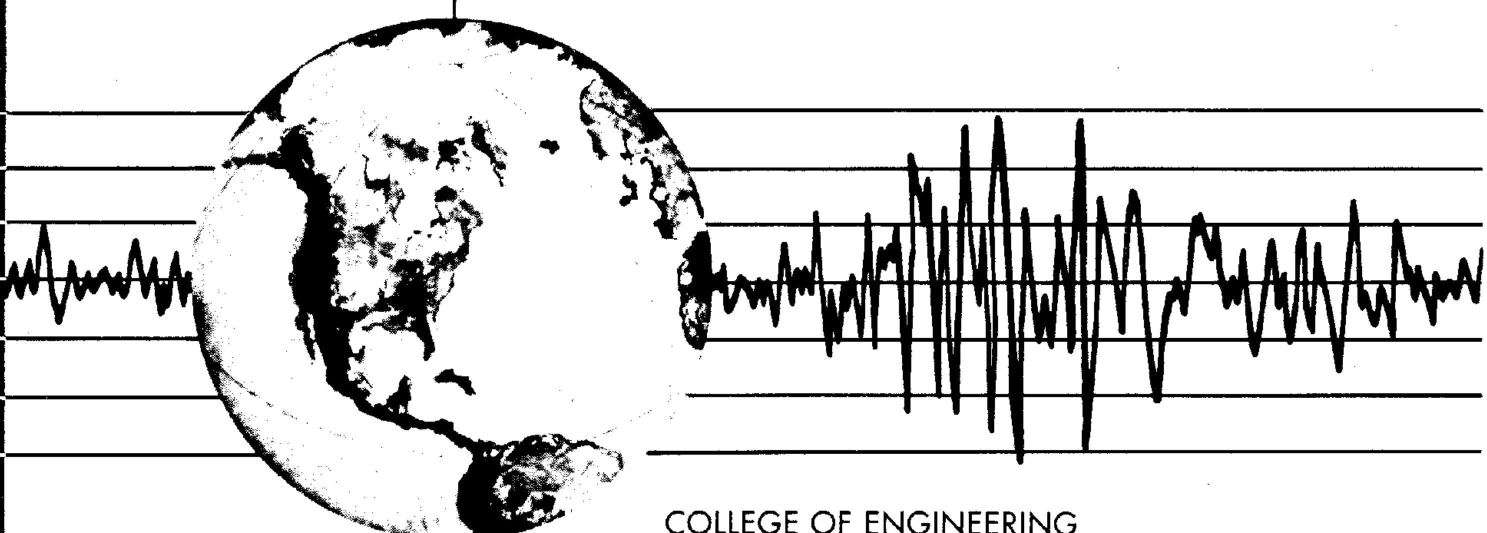

COLLEGE OF ENGINEERING

UNIVERSITY OF CALIFORNIA AT BERKELEY

REPRODUCED BY: NTIS
U.S. Department of Commerce
National Technical Information Service
Springfield, Virginia 22161

For sale by the National Technical Information Service, U.S. Department of Commerce, Springfield, Virginia 22161

See back of report for up to date listing of EERC reports.

DISCLAIMER

Any opinions, findings, and conclusions or recommendations expressed in this publication are those of the authors and do not necessarily reflect the views of the Sponsors or the Earthquake Engineering Research Center, University of California at Berkeley.

PB96-143177

Behavior of Pre-Northridge Moment Resisting Steel Connections

by

Tzong-Shuoh Yang
and
Egor P. Popov

Report to Sponsors:
National Science Foundation
American Institute of Steel Construction

Report No. UCB/EERC-95/08
Earthquake Engineering Research Center
College of Engineering
University of California at Berkeley

August, 1995

PROTECTED UNDER INTERNATIONAL COPYRIGHT
ALL RIGHTS RESERVED.
NATIONAL TECHNICAL INFORMATION SERVICE
U.S. DEPARTMENT OF COMMERCE

REPORT DOCUMENTATION PAGE

Form Approved
OMB No. 0704-0188

Public reporting burden for this collection of information is estimated to average 1 hour per response, including the time for reviewing instructions, searching existing data sources, gathering and maintaining the data needed, and completing and reviewing the collection of information. Send comments regarding this burden estimate or any other aspect of this collection of information, including suggestions for reducing this burden, to Washington Headquarters Services, Directorate for Information Operations and Reports, 1215 Jefferson Davis ... and to the Office of Management and Budget, Paperwork Reduction Project (0704-0188), Washington, DC 20503.

1. PB96-143177

2. REPORT DATE: August 1995

3. REPORT TYPE AND DATES COVERED: Final

4. TITLE AND SUBTITLE
Behavior of Pre-Northridge Moment Resisting Steel Connections

5. FUNDING NUMBERS

6. AUTHOR(S)
Yang, Tzong-Shuoh and
Popov, Egor P.

7. PERFORMING ORGANIZATION NAME(S) AND ADDRESS(ES)
Earthquake Engineering Research Center
University of California at Berkeley
1301 S. 46th Street
Richmond, CA 94804

8. PERFORMING ORGANIZATION REPORT NUMBER
UCB/EERC-95/08

9. SPONSORING/MONITORING AGENCY NAME(S) AND ADDRESS(ES)
National Science Foundation
1800 G Street, N.W.
Washington, D.C. 20550

American Inst of Steel Construction
1 East Wacker Dr, Ste 3100
Chicago, IL 60601-2001

10. SPONSORING/MONITORING AGENCY REPORT NUMBER

11. SUPPLEMENTARY NOTES

12a. DISTRIBUTION/AVAILABILITY STATEMENT

12b. DISTRIBUTION CODE

13. ABSTRACT (Maximum 200 words)

The basic reasons for the fractures that occurred in steel moment-resisting connections during the 1994 Northridge earthquake are examined from a fundamental point of view. This examination begins with a discussion of material properties, and calls attention to the shortcomings of the conventional tension test. The stress-strain diagrams for specimens having a circular groove around the specimen (resembling a condition at the critical weld at a connection) are entirely different, exhibiting a brittle fracture compared with a ductile response for a bar of constant cross-section. The misleading ASTM requirement for minimum strength with no specified maximum results in a melee of actual strengths in use of which the designer is unaware. This prevailing condition makes it impossible to design rationally.

14. SUBJECT TERMS

15. NUMBER OF PAGES: 63

16. PRICE CODE

17. SECURITY CLASSIFICATION OF REPORT	18. SECURITY CLASSIFICATION OF THIS PAGE	19. SECURITY CLASSIFICATION OF ABSTRACT	20. LIMITATION OF ABSTRACT
unclassified	unclassified	unclassified	

Abstract

The basic reasons for the fractures that occurred in steel moment-resisting connections during the 1994 Northridge earthquake are examined from a fundamental point of view. This examination begins with a discussion of material properties, and calls attention to the shortcomings of the conventional tension test. The stress-strain diagrams for specimens having a circular groove around the specimen (resembling a condition at the critical weld at a connection) are entirely different, exhibiting a brittle fracture compared with a ductile response for a bar of constant cross-section. The misleading ASTM requirement for minimum strength with no specified maximum results in a melee of actual strengths in use of which the designer is unaware. This prevailing condition makes it impossible to design rationally.

Next, the possible modes of failure are examined, showing the very limited view in the code design. Then, a simplified and more accurate analysis of the beam-column connection is examined.

Based on the above background, three SAC Pre-Northridge specimen tests subjected to cyclic loading are critically examined. Good comparisons are found using the above theory. However, the effect of the backing bars on the capacity of the connection need to be studied in more detail.

Recognizing that the unfused material between a column face and a backing bar forms an "artificial" edge crack, the methods of nonlinear finite element analysis combined with fracture mechanics were brought to bear. In the finite element analysis, the backing bar became one of the parts in a three-dimensional model of the connection. Using these procedures, it was possible to predict the instant of fracture, and to construct analytically complete hysteretic loops for the specimens. Remarkable agreement between these loops and experimental ones was achieved.

It is interesting that one of the two identical specimens fractured at a smaller tip load applied to the cantilever on a cold, murky day. This was predicted by the fracture mechanics theory, as the ambient temperature on that day was about 10°F lower than during the test with the other specimen.

The report concludes by clearly showing that, at higher applied loads, the bottom backing bar develops decidedly higher stresses at the column face than does the upper backing bar. These studies also indicate that, instead of removing the backing bars and applying a closure weld, a less expensive method of sealing the vertical "artificial" crack with a small weld may be almost equally effective.

Introductory Remarks

Because of the urgency created by the January 17, 1994 Northridge earthquake, which caused numerous failures of steel-moment resisting connections in buildings, this report is released based on the as yet unpublished doctoral dissertation of Tzong-Shuoh Yang, prepared under the supervision of Egor P. Popov. It is the belief of the authors that this information should be made available to structural engineers and code formulating authorities at the earliest possible date.

Acknowledgements

The authors are most grateful to Drs. S.-C. Liu and M. P. Singh of NSF for encouraging this study and providing the necessary funds for carrying out the work. The authors also sincerely thank Nestor Iwankiw of AISC for providing supplementary funds and arranging for delivery at no cost of several tons of steel to proceed with the experimental phase of the project.

Gratis fabrication of very large specimens for validating some of the analyses, made-up by PDM Strocal, Inc. with Fred Long in charge, and by the Herrick Corporation with Vice-President Roger Ferch, were essential for the success of the project.

The availability of data from the SAC experiments was necessary for some formulations. In this regard the cooperation of Stephen A. Mahin of SAC and UCB as well as of James O. Malley of SAC and Degenkolb Engineers is also greatly appreciated.

The kindness of Professor Albert P. Pisano of the Mechanical Engineering Department deserves special mention, as he provided access to his powerful computer facilities for the extensive analyses presented in this report.

Contents

List of Figures

List of Tables

Introduction

Before the 1994 Northridge earthquake, steel moment-resisting frames (MRFs) were considered ductile by engineers. The dream was broken suddenly after the earthquake. Many brittle failures were reported throughout the greater Los Angeles area [6, 30]. Most serious fractures occurred at the welded beam-to-column connections. This has called into question the strength and ductility of such connections.

This report presents the analytical studies of pre-Northridge welded beam-to-column connections used in typical steel MRFs. In the analysis, no defects in welding material, welding procedure, or workmanship are assumed. The purpose of these studies is to give explanations for both fracture locations and failure modes of the aforementioned connections in quantitative and rational ways. The stress concentration at the juncture of a welded beam flange and a column flange is analyzed by three-dimensional elastic-plastic finite elements based on the von Mises yield criterion with associated plastic flow. The results clearly explain that the weak beam flange breaks off right at the weld due to triaxial state of stress in this region. The important effect of the weak column panel zone was not fully explored before. In this report, it is shown that the column web fractures are closely related to the weak panel zone. The important effect of the backing bar in the connection failure is analyzed next by fracture mechanics methods. The unfused backing bar side next to the column flange is interpreted as an artificial crack. Flange tension due to bending of the beam opens the artificial crack between the backing bar and the column flange, and initiates the rupture. The stress-intensity factors at the artificial crack tips of both top and bottom backing bars are calculated by the J-integral method. The results clarify why the rupture generally was initiated at the bottom flange but not at the top flange. Finally, the analytical cyclic load-deflection curve and plastic energy dissipation are compared with the three SAC[1] Joint Venture full-size specimens tested at the University of California at Berkeley. Good agreement between the analytical results and the experimental tests conclude the report.

[1]SAC is an acronym for Structural Engineers Association of California, Applied Technology Council, and California Universities for Research in Earthquake Engineering.

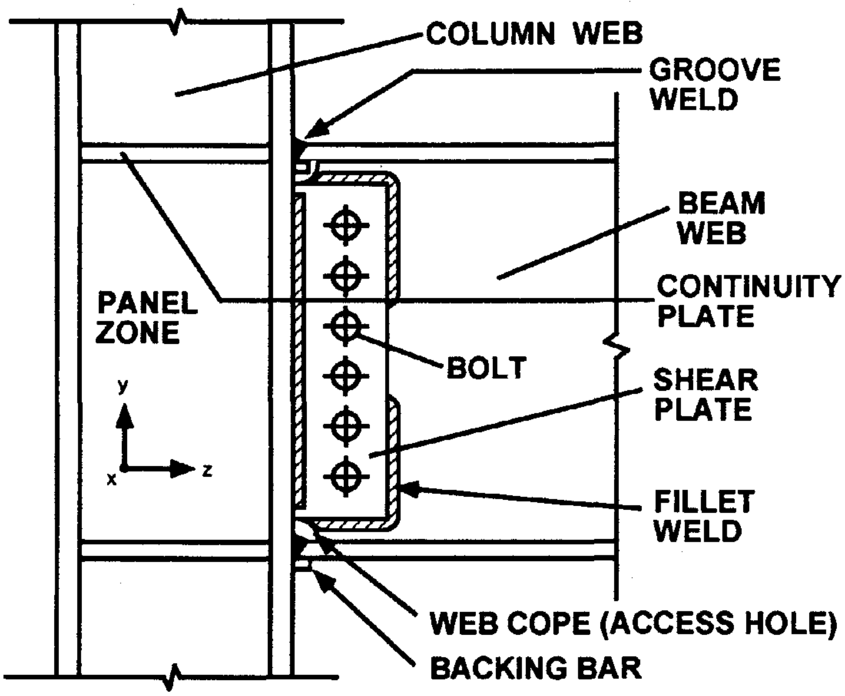

Fig. 1: A typical welded beam-to-column connection.

Material Properties of Structural Steel

A typical welded beam-to-column moment resisting connection is shown in Fig. 1. The top and bottom flanges of the beam are welded directly to the column by full penetration groove welds. The beam web is bolted or welded to a shear plate, which is attached to the column by welding. The most serious rupture modes of such connections are shown in Fig. 2. The failure modes are catastrophic because they fracture at extremely high speeds without exhibiting prior ductile behavior. This violates the precept of the ductile MRF.

Before studying the non-ductile failure of the connection, some remarks on the material properties need to be made. The stress-strain curve of a small diameter uniform cylindrical steel (bar (a) in Fig. 3) loaded longitudinally to failure, will be ductile (curve (a) in Fig. 3). A small diameter bar of uniform cross-section is not restrained in the lateral direction, and allows Poisson contraction, which leads to specimen necking down and develops shear slip layers (Lueders lines) during failure. However, for a cylindrical bar with a groove or notch, such as bar (b) in Fig. 3, even though the cross sectional area at the groove is the same as bar (a), the tensile stress-strain curve is completely different. When loaded in tension, the grooved part will

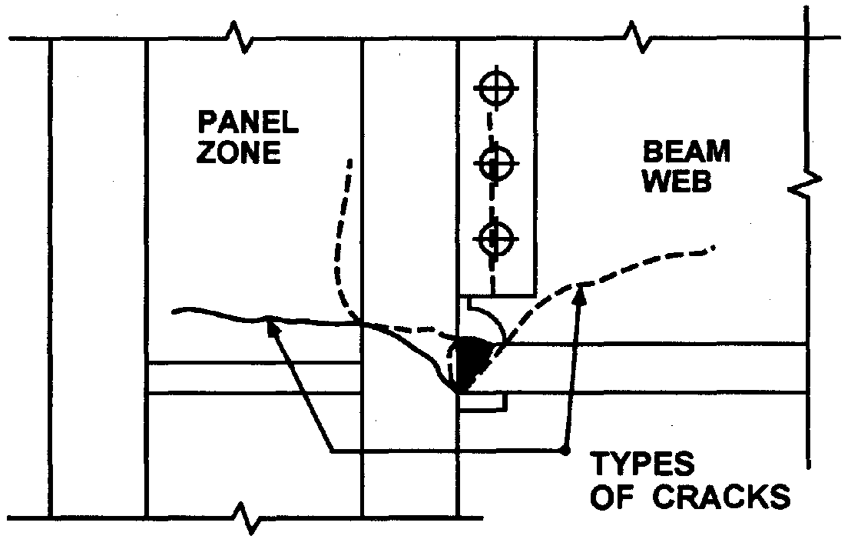

Fig. 2: Some failure modes of the welded beam-to-column connection.

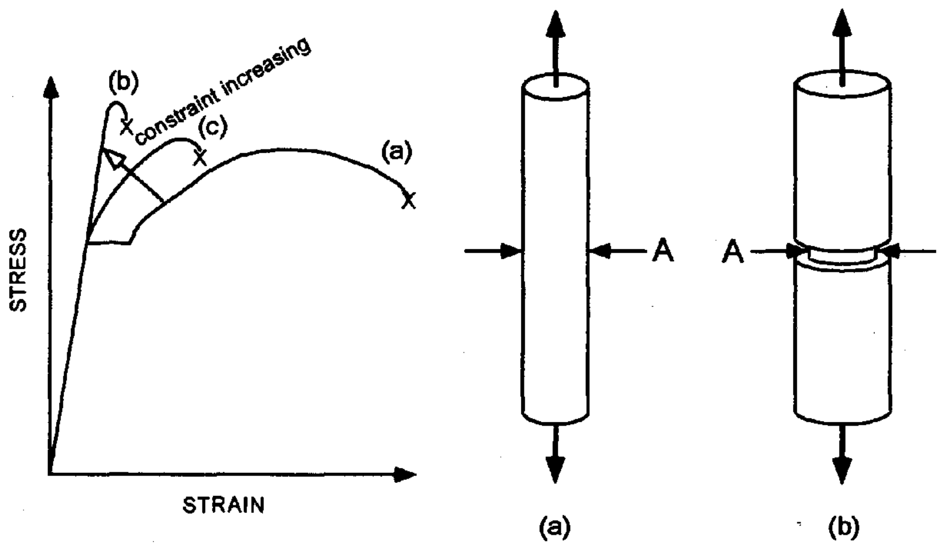

Fig. 3: Simple tensile test of steel specimens with the same critical cross section area: (a) cylindrical bar, and (b) grooved cylindrical bar.

have the largest stress, but due to the constraint of the larger sections outside the groove, no lateral contraction or shear flow can develop at the groove. The failure of bar (b) is caused by triaxial tension resulting in a brittle failure with no apparent yielding. The stress at breaking is near the cohesion strength of the material; its stress-strain curve is similar to curve (b) in Fig. 3. Timoshenko on page 435 of his book says [28]:

> Because most of the grooved specimen remains elastic during a tensile test to failure, it will have a very small elongation, and hence only a small amount of work is required to produce fracture. A small impact force can easily supply the work required for failure. The specimen is brittle because of its shape not because of any mechanical property of the material.

There were many research studies on grooved specimens, i.e. Kirkaldy [16], Ludwik and Scheu [17], and MacGregor [18]. Stress concentration factors for a variety of grooved bars can be found, for example, in Neuber [19] and Peterson [21].

It can be seen in Fig. 1 that the welded beam flange cannot be deformed in both x and y directions because it is welded to a relatively large column flange with continuity plates. The welded beam flange also has to resist the largest bending moment caused by the loads on its span and frame drift. The stress on the beam flange outside the weld is smaller because of reduced moment and lesser lateral strain constraint. The welded beam-to-column connection has the strain constraint and the largest stress, which make it essentially like a grooved bar except of different shape. It can be expected that the tensile stress-strain curve right at the beam flange weld will be between curves (a) and (b) in Fig. 3 depending on the degree of constraint, web cope (access hole) size, and bending moment gradient.

Another important fact regarding the mechanical properties of today's steel is that the yield strength of A36 steel is no longer 36 ksi. Fig. 4 shows a series of tested stress-strain curves of coupons cut from A36 W12×26 beams. The average yield strength of A36 steel is about 48 ksi, the ultimate strength of A36 steel is about 70 ksi.

Table 1 lists *minimum* yield strength, F_y, and minimum ultimate strength, F_u, for certain ASTM steels given in the AISC specifications. The ANSI-ASTM standard B483-78 defines minimum strength as follows:

> Standard mechanical property limits for the respective size ranges are based on an analysis of data from standard production material and are

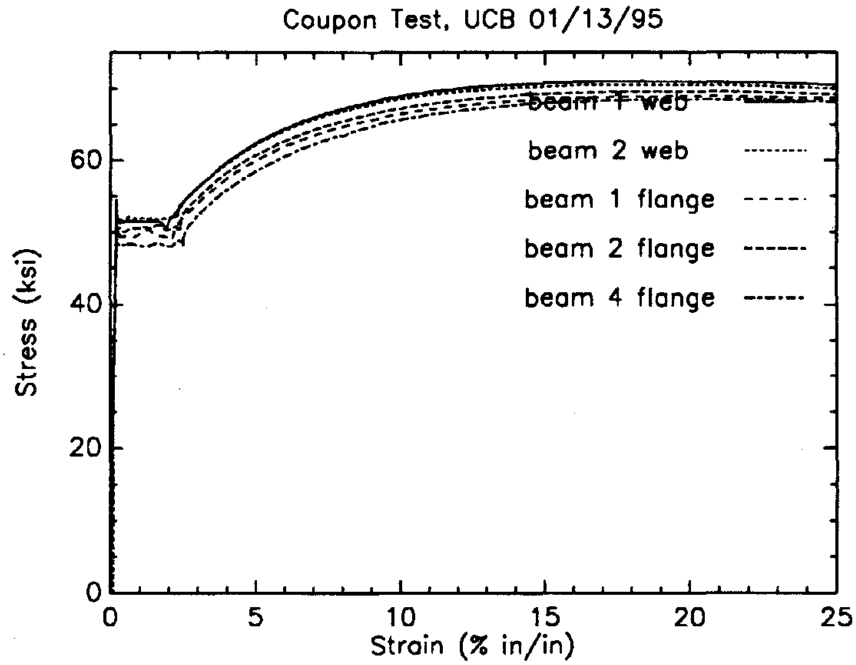

Fig. 4: Stress-strain curves of a series of tensile tests for A36 steel.

ASTM Number	A36	A592	A572 Gr50	A588	A514
Steel Type	Carbon	Carbon	Low alloy	Stainless	Alloy Q&T†
Minimum F_y (ksi)	36	42	50	50	100
Minimum F_u (ksi)	58	60	65	70	110

†Q&T: Quenching and Tempering

Table 1: Specified minimum strengths of certain ASTM steels.

> established at a level [at] which at least 99 percent of the production of values obtained from all standard material in the size range meets the established value.

The unqualified word *minimum* may be misleading, since there is a chance that the materials involved may have a strength much higher than the minimum. In the statement, there is no specification for the upper bound of steel strength. For structural elements loaded to the allowable stress level, the statement is adequate for design. However, in seismic resisting structures, many elements can be stressed beyond the yield strength during a strong earthquake to develop the needed ductile behavior. The ASTM specifications provide no information for designers to control deformation because the material strength can be much higher than the minimum value. The A36 materials tested in the laboratory have an average yield strength 33% over the specified minimum value (Fig. 4). Such high variance on strength makes stress analysis meaningless.

The AISC specification states that:

> Certified mill test reports or certified reports of tests made by the fabricator or a testing laboratory in accordance with ASTM A6 or A568, as applicable, and the governing specification shall constitute sufficient evidence of conformity with one of the ASTM standards. Additionally, the fabricator shall, if requested, provide and affidavit stating that the structural steel furnished meets the requirements of the grade specified.

The AISC statement ensures that materials having these minimum strengths are actually used in the construction, but the designers have no way to know the actual material strengths during design until the materials reach the fabrication stage.

A more appropriate material specification would be to give the average material strength with a specified small variance. Designers can use the average as the nominal design value and use the variance for reliability analysis.

Design Strategy

The most essential characteristic of MRF is the requirement that plastic hinges be formed near connections during severe loading conditions. These plastic hinges provide strength and ductility to dissipate energy hysteretically. As was stated earlier, it is impossible to develop large plastic deformation right at the beam-column weld

Failure Type	Minimum Capacity	Failure Mode
1	C_m^b or C_v^b	beam flange or shear plate rupture (crack 3 in Fig. 6)
2	C_m^c or C_v^c	fracture through column web or divot pullout from column flange (crack 1 or 2 in Fig. 6)
3	C_{cr}^b	buckling of beam near connection and formation of plastic hinge (weak beam-strong column connection)
4	C_{cr}^c	buckling of column near connection and formation of plastic hinge (strong beam-weak column connection)

Table 2: Four possible failure types of a steel MRF connection.

location. Thus, the plastic hinges can only be formed at the beam or column section near the connection.

In oder to establish the design strategy, let the resisting capacity at the connection be defined by the following symbols:

$$
\begin{aligned}
C_m^b &= \text{Moment resisting capacity of beam at the connection} \\
C_v^b &= \text{Shear resisting capacity of beam at the connection} \\
C_m^c &= \text{Moment resisting capacity of column at the connection} \\
C_v^c &= \text{Shear resisting capacity of column in the panel zone} \\
C_{cr}^b &= \text{Local buckling strength of beam near the connection} \\
C_{cr}^c &= \text{Local buckling strength of column near the connection}
\end{aligned}
$$

The superscripts b and c are used to designate *beam* and *column*, respectively. The actual resisting capacity of a connection is controlled by the minimum of these six values[2]. The minimum resisting capacity is based on the failure type. The four possible failure types are given in Table 2. In this table, Types 1 and 2 correspond to sudden fractures and should be avoided. By developing plastic hinges near the connections, Type 3 and 4 mechanisms assure good strength and ductility (Fig. 5). For beam flange connections welded directly to the column flange, the resisting capacity C_m^b is always smaller than the ultimate moment capacity of the beam. In such a situation, in order to develop a Type 3 mechanism, a non-compact beam section must be

[2]The resisting capacity is also affected by backing bars at the welds. This will be discussed later.

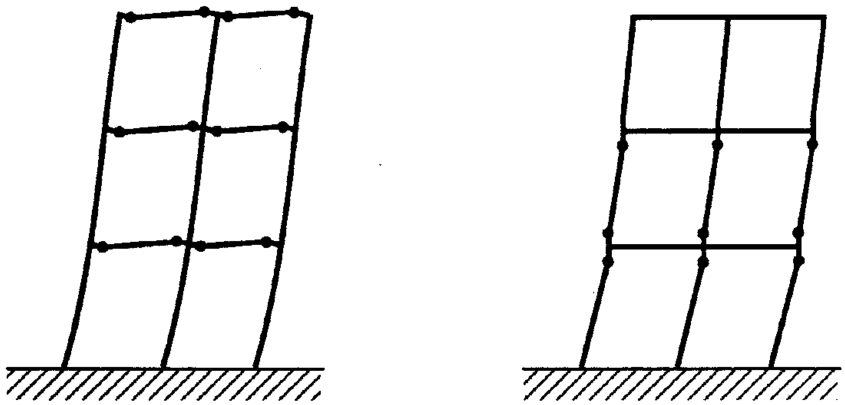

Fig. 5: Two alternative plastic hinge mechanisms for a typical MRF: (a) Type 3 mechanism and (b) Type 4 mechanism.

used. The derivations for C_m^b and C_{cr}^b are given in the next section. It is to be noted that the kinematic mechanisms shown in Fig. 5 are associated with early inelastic action and do not represent collapse mechanisms.

Simplified Stress Analysis

In the linear elastic range, the stress in the z direction at the outer-most fiber point A, shown in Fig. 6 near the weld to the connection, is denoted as σ_{zz}^A. The nominal value of σ_{zz}^A can be calculated from

$$\sigma_{zz}^A = \frac{M}{S_x^b} \tag{1}$$

where M is the applied bending moment, and S_x^b is the section modulus of the beam. The corresponding strain is expressed as

$$\epsilon_{zz}^A = \sigma_{zz}^A / E \tag{2}$$

where E is the Young's modulus of the beam.

Point A is not constrained by the weldment. On the other hand, point B is also at the outer-most fiber of the beam at the center of the beam-column junction. As shown in Fig. 6, point B is restrained by the weldment, which is directly attached to a wide thick column flange and cannot displace in either the x or y direction, hence $\epsilon_{xx}^B = \epsilon_{yy}^B = 0$. The stress state of point B is in the transition zone from plane stress

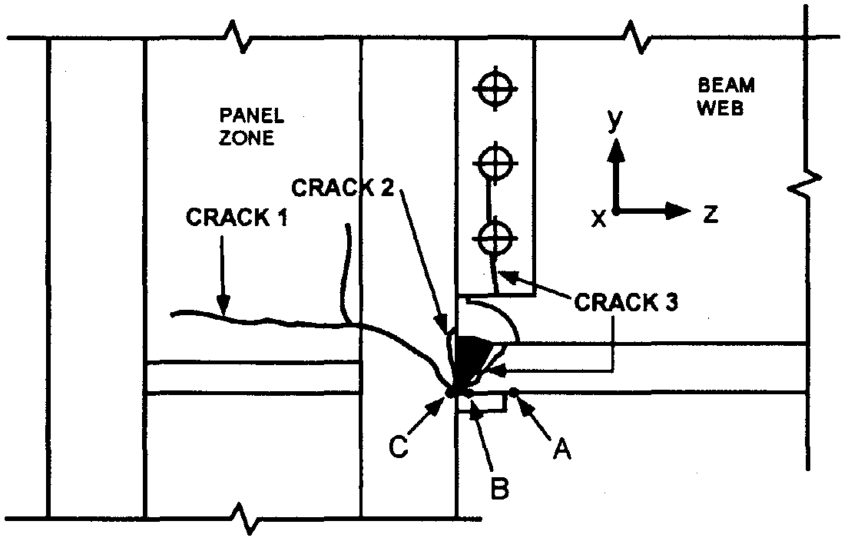

Fig. 6: Critical points in the connection - point A on beam flange, point B on beam-weldment junction, and C at column flange.

to plane strain. Because point B is so close to point A, its strain ϵ_{zz}^{B} in direction z can be assumed to be equal to ϵ_{zz}^{A}, and the stresses at point B can then be determined by Hooke's law:

$$\sigma_{zz}^{B} = \frac{(1-\nu)E}{(1+\nu)(1-2\nu)}\epsilon_{zz}^{B} = \frac{(1-\nu)E}{(1+\nu)(1-2\nu)}\epsilon_{zz}^{A} = \frac{(1-\nu)}{(1+\nu)(1-2\nu)}\sigma_{zz}^{A} \quad (3)$$

$$\sigma_{xx}^{B},\ \sigma_{yy}^{B} = \frac{\nu E}{(1+\nu)(1-2\nu)}\epsilon_{zz}^{B} = \frac{\nu E}{(1+\nu)(1-2\nu)}\epsilon_{zz}^{A} = \frac{\nu}{(1+\nu)(1-2\nu)}\sigma_{zz}^{A} \quad (4)$$

where ν is Poisson's ratio. Since for steel, $\nu = 0.3$ and $E = 29,000$ ksi, approximately, the above equations reduce to

$$\sigma_{zz}^{B} = 1.35\sigma_{zz}^{A} \quad (5)$$

$$\sigma_{xx}^{B},\ \sigma_{yy}^{B} = 0.58\sigma_{zz}^{A} \quad (6)$$

To verify the adequacy of the estimated stress concentration factors derived above, a series of elastic finite element analyses was performed based on the geometry of the SAC specimen (see next section) by varying the column flange thickness while keeping the beam flange thickness constant. The results are shown in Fig. 7. The stress concentration factor of each component of stress is plotted against the beam/column flange thickness ratio. The stress concentration factors of σ_{zz} range from 1.2 to 1.46, which is very close to the calculated simplified value of 1.35, but the stress concentration factors for σ_{xx} and σ_{yy} are much less than the estimated value 0.58. The lower

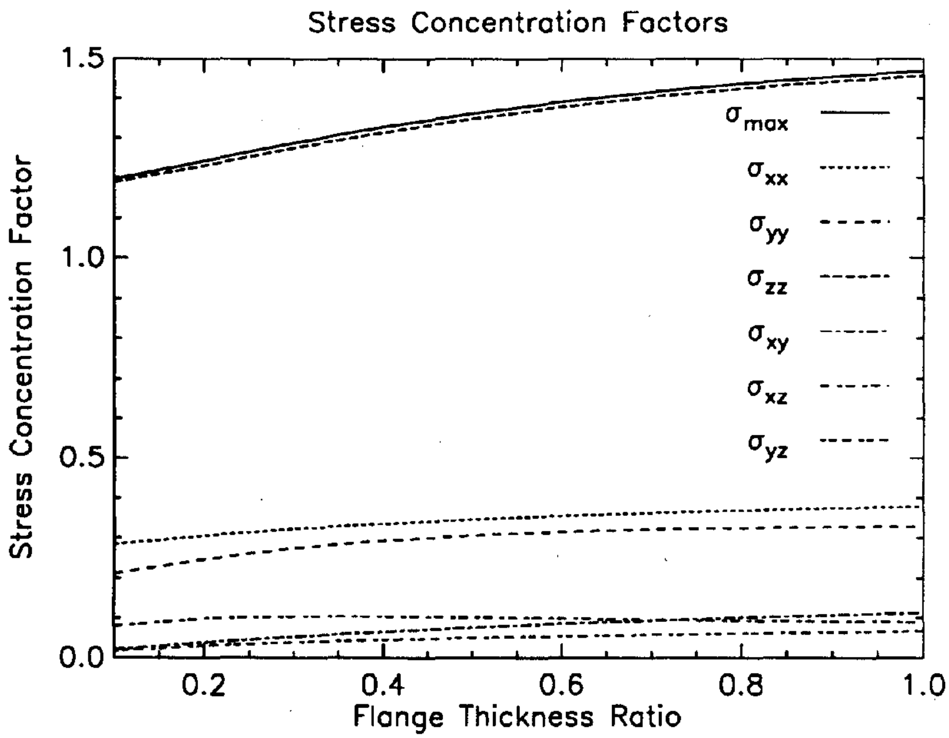

Fig. 7: Stress concentration factors at juncture of beam-to-column connection calculated by elastic finite element analysis. The external load is uniformly distributed unit tensile stress σ_{zz} applied on the beam flange.

three curves in the figure show how small the flange shear stresses are at the juncture. Because of the low shear stresses, no shear slip can form, resulting in no ductility. For the same reason, the beam fracture is governed by the maximum-normal-stress criterion. The maximum-normal-stress criterion states that failure occurs whenever one of the three principal stresses equals the uniaxial material strength. The maximum principal tension stress σ_{max} of the beam flange at the juncture of the beam-column connection is plotted in Fig. 7, which is very close to the σ_{zz} curve.

In the inelastic range, the stress across the flange will re-distribute to become much more evenly distributed, although the greatest stress value remains at the flange center. All rolled steel members (W, M, C, etc.) possess residual stresses due to differential cooling. The flange tips and interior web parts always cool more quickly than the other parts of the flange. In this manner, the flange tips develop compressive stresses, while the residual stresses are tensile in the middle of the flange.

The yielding moment of a member can be calculated with a sufficient degree of accuracy by the following equation

$$M^b_{yield} = (F_y - F_r)S^b_x \tag{7}$$

where F_r is the maximum compressive residual stress in either flange tip of the beam. The average compressive residual stress at the flange tips of small to medium size rolled shapes is about 13 ksi for A36 steel with 36 ksi yield strength [5, 10]. It is reasonable therefore to assume that the value of the residual stress is a fraction of the yield strength

$$F_r = \frac{13}{36}F_y = 0.36F_y \tag{8}$$

The residual stresses for large hot-rolled sections can be found in Alpsten [1]. The plastic moment capacity of a rolled section is hardly affected by the presence of residual stresses and can be calculated simply as

$$M^b_{plastic} = F_y Z^b_x \tag{9}$$

where Z^b_x is the plastic modulus of the beam. The ultimate moment capacity of a beam can be reached by bending a plastic section into the strain-hardening range. Hence the ultimate bending capacity is expressed as

$$M^b_{ultimate} = F_u Z^b_x \tag{10}$$

For a directly welded beam-to-column connection without cover plate, the bending beam moment is transferred primarily through the beam flanges into the column regardless of the size of the shear plate. The ultimate moment capacity of the connection therefore can be calculated by

$$C_m^b = F_u Z_f^b \tag{11}$$

where Z_f^b is the plastic modulus of the beam flanges. Because Z_x^b is larger than Z_f^b, the ultimate moment capacity of the beam $M_{ultimate}^b$ is always larger than the connection moment capacity C_m^b. If the rolled shape section is compact, no local buckling will occur before $M_{ultimate}^b$ is reached, and the rapid failure occurs by tearing off the flange.

The local buckling stress of a beam flange can be derived from the plate buckling stress. In general, the plate buckling stress in the elastic range is given by

$$\sigma_{cr} = k\frac{\pi^2 E}{12(1-\nu^2)}\left(\frac{t}{b}\right)^2 \tag{12}$$

where t and b are the thickness and the width of the plate, respectively. k is the plate buckling coefficient, which depends on the plate geometry and boundary conditions. For the beam flange of a wide-flange rolled shape, k is 0.7. The plate buckling stress in the inelastic range can be shown to be [8]

$$\sigma_{cr} = k\frac{\pi^2 \sqrt{EE_t}}{12(1-\nu^2)}\left(\frac{t}{b}\right)^2 \tag{13}$$

where E_t is the tangent modulus of the material. From the buckling stress, the critical beam moment capacity C_{cr}^b can be calculated from

$$C_{cr}^b = \sigma_{cr} Z_f^b \tag{14}$$

To safely design a beam-column connection, it is desirable that

$$C_{cr}^b \ < \ C_m^b \ < \ M_{ultimate}^b \tag{15}$$

But for economic use of the material, the critical stress should obey the following relation

$$F_y \leq \sigma_{cr} < F_u \tag{16}$$

Three SAC Pre-Northridge Specimen Tests

In order to help understand the strength and ductility of the welded moment resisting connections, three specimens have been fabricated according to the standards used

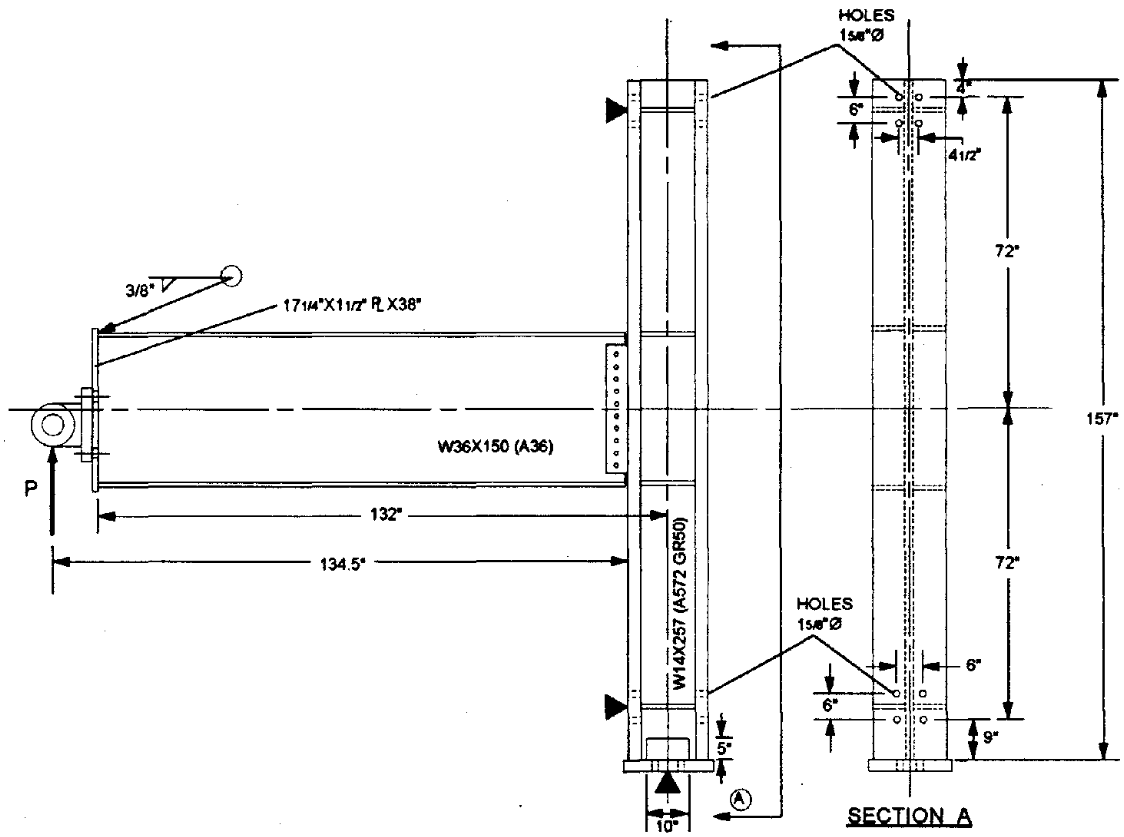

Fig. 8: Detail of the SAC PN specimens.

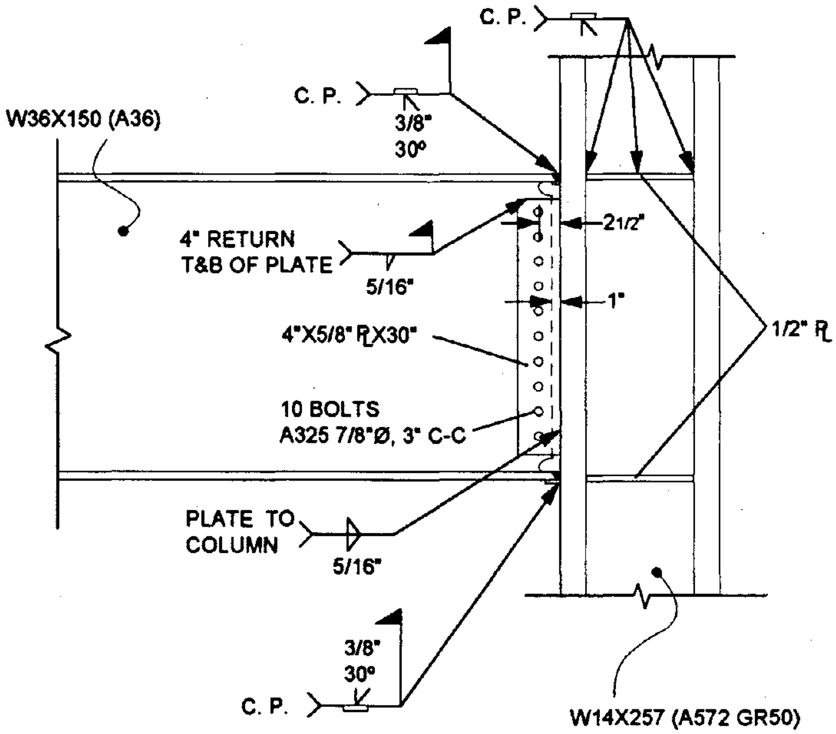

Fig. 9: Connection detail for SAC PN specimens.

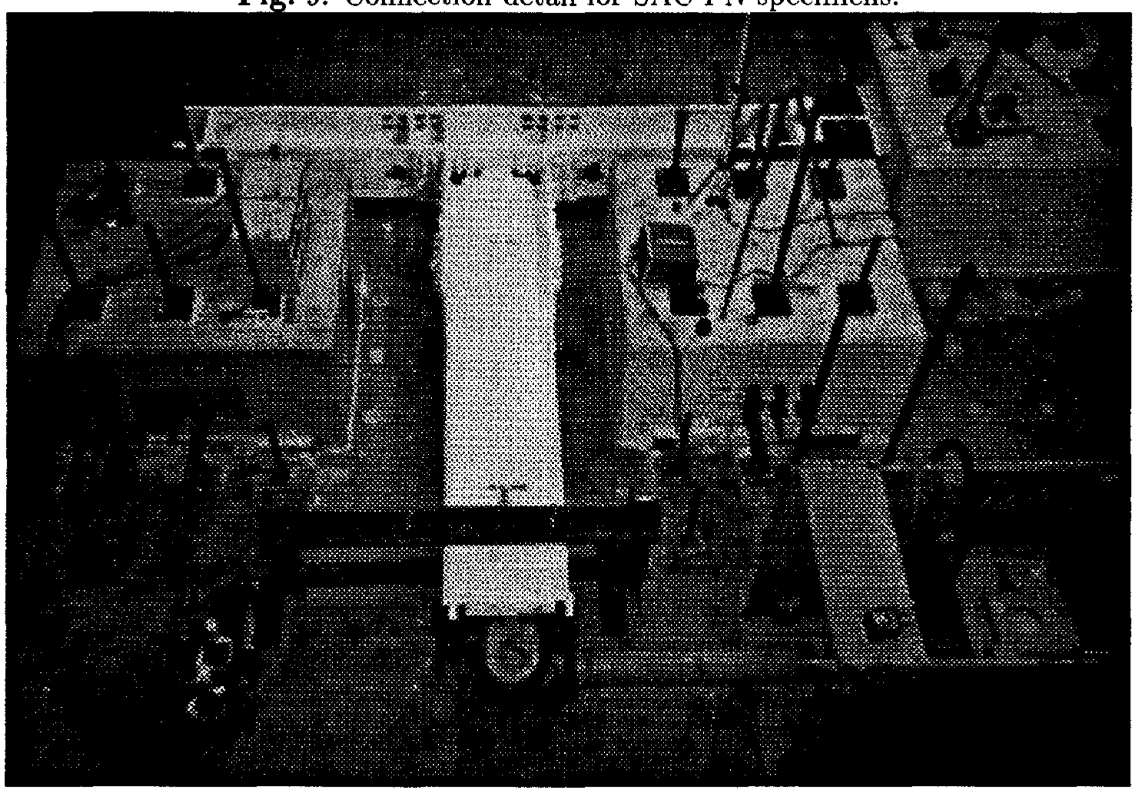

Fig. 10: Photograph showing specimen tested horizontally in laboratory. Left side of the beam is the *upper* side of the specimen.

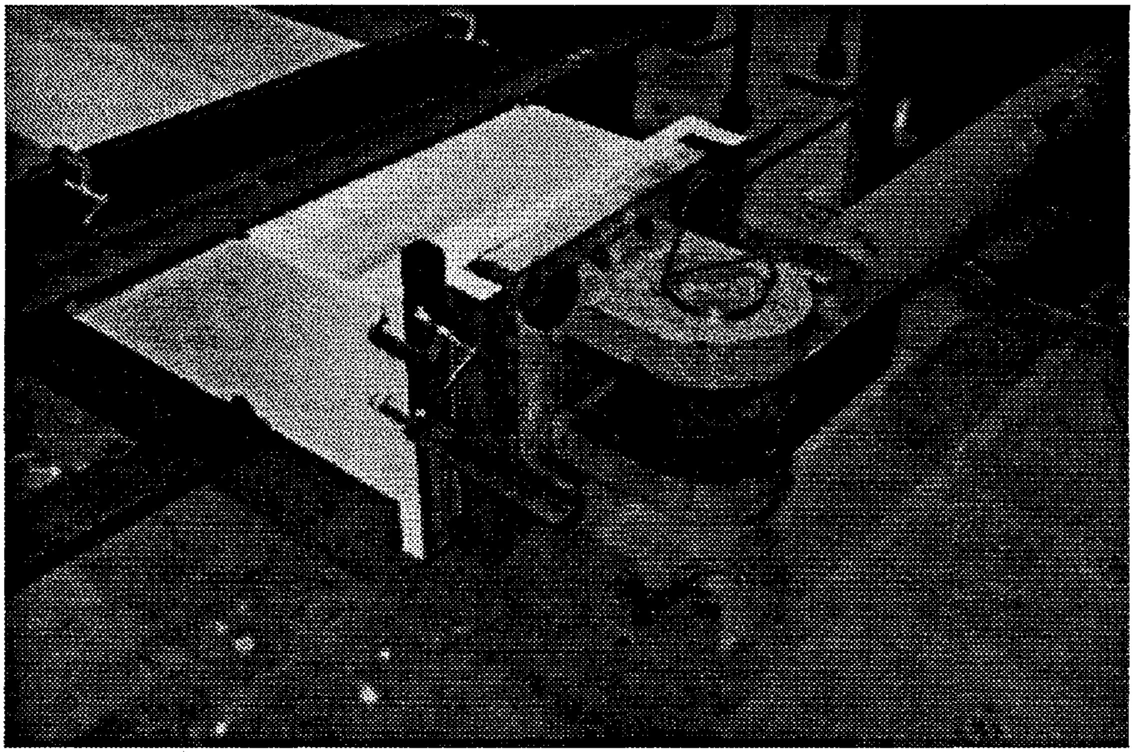

Fig. 11: Photograph showing the clevis connected to beam end-plate and hydraulic actuator.

before the 1994 Northridge earthquake. These were tested at UC Berkeley under the guidance of the SAC Joint Venture. The dimensions of these specimens are shown in Fig. 8. The connection detail is shown in Fig. 9. These specimens were tested in a horizontal position. The test setup is shown in Fig. 10. An end-plate is welded to the cantilever beam and bolted to a clevis, which connects to a computer-controlled 350 kips hydraulic actuator (see Fig. 11). Slowly varying cyclic loads are applied to the beam tip by the actuator. The column is simply supported at the ends by prestressed rods tightened to three reinforced concrete blocks. These reaction blocks are prestressed to the floor by high-strength rods. The reaction and loading points simulate the inflection points occurring in mid span of a frame. At the top of the column, in order to simulate a roller support at the end, the column is tightened to a reaction block by four prestressing rods (Fig. 12). At the bottom of the column, in order to simulate a hinged end, the column is tightened to the reaction blocks by prestressed rods in two directions (Fig. 13). Detailed information of the setup can be found in the thesis by Blackman [7]. During the fabrication of the specimens, two A572-Gr50 beams were mistakenly used in the first two specimens PN1 and

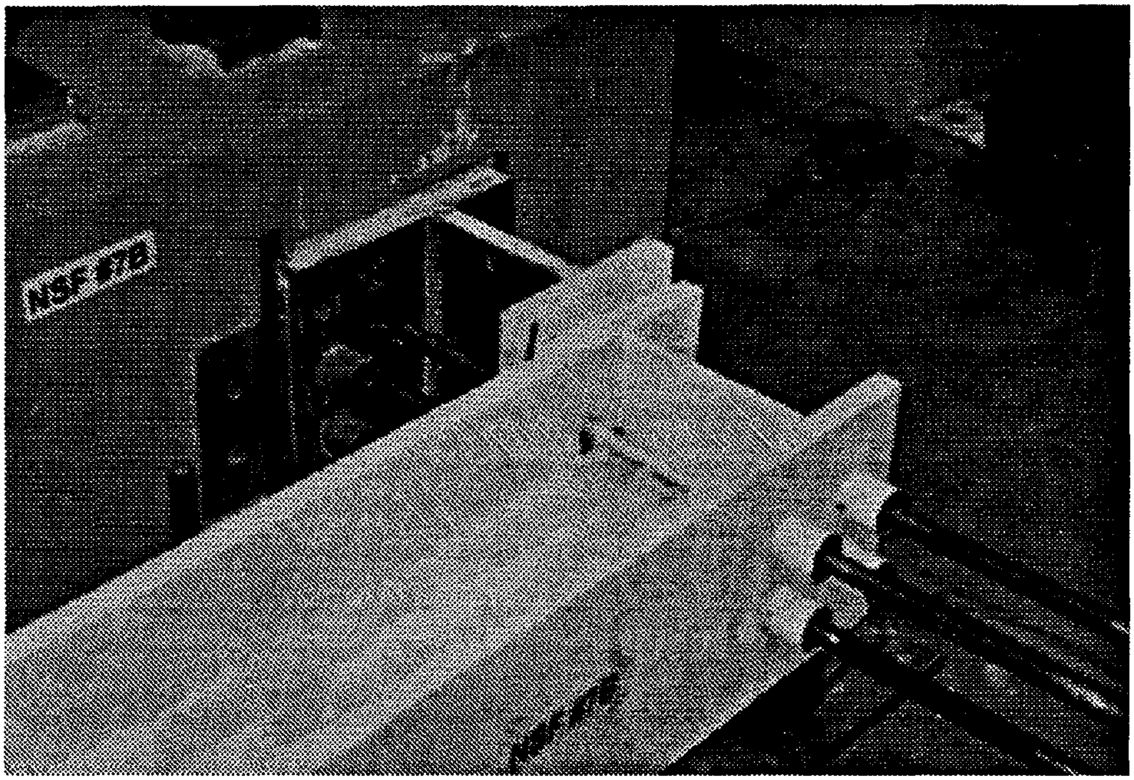

Fig. 12: Photograph showing the top of the column.

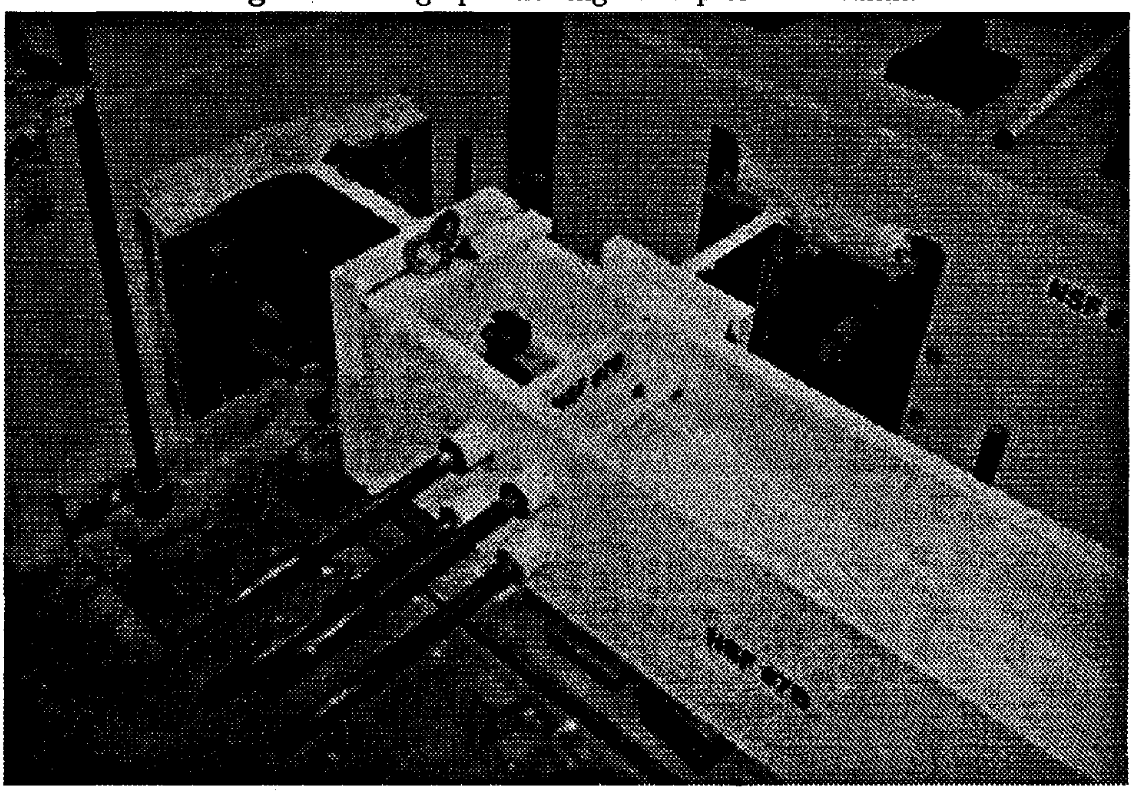

Fig. 13: Photograph showing the bottom of the column.

Material Properties
(from Mill Certificates)

Specimen Number	Material Size & Spec	Yield Strength F_y (Elongation)	Ultimate Strength F_u (Elongation)
PN1, PN2 & PN3 Column	W14×257 A572-Gr50	53.5 ksi (0.18%)	72.5 ksi (N/A)
PN1 & PN2 Beam	W36×150 A572-Gr50	62.6 ksi (0.22%)	74.7 ksi (22.5%)
PN3 Beam	W36×150 A36	56.8 ksi (0.20%)	68.7 ksi (28.0%)

Table 3: Material properties of the SAC Joint Venture PN specimens.

PN2. Only the third specimen PN3 was made of the correct materials. The material properties of these three specimens as determined from mill certificates, and are given in Table 3. Notice that the yield strength of A572 Grade 50 PN1 and PN2 beam is 25% over the ASTM minimum, the yield strength of the A36 PN3 beam is 58% over the ASTM minimum. The high scatter in material strengths may result in inadequate structures.

Each SAC specimen has a cantilever beam with a concentrated force P applied at its free end (see Fig. 8). The arm length L of the concentrated force to the face of the column flange is 134.5 inches. The moment capacities of these specimens can be calculated by Eqs. 7-11. The corresponding concentrated forces can also be calculated by dividing the moment by the moment arm. For PN1 and PN2 specimens, the yield force can be calculated as

$$P_{yield} = M^b_{yield}/L = S^b_x(F_y - F_r)/L = 504(62.6 - 0.36 \times 62.6)/134.5 = 150 \text{ kips} \tag{17}$$

and the peak force can be calculated as

$$P_{peak} = C^b_m/L = Z_f F_u/L = 392.96 \times 74.7/134.5 = 218 \text{ kips} \tag{18}$$

Similarly, the yield and peak forces of the PN3 specimen can be calculated as

$$\begin{aligned} P_{yield} &= S^b_x(F_y - F_r)/L = 504(56.8 - 0.36 \times 56.8)/134.5 = 136 \text{ kips} && (19) \\ P_{peak} &= C^b_m/L = Z_f F_u/L = 392.96 \times 68.7/134.5 = 201 \text{ kips} && (20) \end{aligned}$$

The shear force in the column below and above the connection due to tip load P can be calculated as

$$V^c = P(L + \frac{d^c}{2})/138 = P(134.5 + 16.38/2)/138 = 1.03P \tag{21}$$

where d^c is the depth of the column (refer to Fig. 8). The axial force at the beam flange can be expressed as

$$T^b = \frac{PL}{d^b - t_f^b} = \frac{134.5P}{35.85 - 0.94} = 3.85P \tag{22}$$

where d^b is the depth of the beam and t_f^b is the flange thickness of the beam. Thus the shear force in the panel zone is

$$V^{pz} = T^b - V^c = 2.82P \tag{23}$$

and the shear capacity of the column is

$$C_v^c = 0.95 d^c t_w^c \frac{F_y^c}{\sqrt{3}} = 0.95 \times 16.38 \times 1.175 \times \frac{53.5}{\sqrt{3}} = 565 \text{ kips} \tag{24}$$

where 0.95 is the effective shear area coefficient, t_w^c is the web thickness of the column, and $1/\sqrt{3}$ comes from the von Mises yield criterion. As long as the tip load is over 200 kips, the column will have shear yielding in the panel zone.

The maximum column bending moment occurs at the section outside the panel zone. Its value is

$$M^c = V^c(69 - d^b/2) = 52.8P \tag{25}$$

The moment capacity of the column is

$$C_m^c = F_u^c Z_x^c = 72.5 \times 542 = 39,300 \text{ kip-in} \tag{26}$$

The column is very safe in bending. The shear plate of the connection is very well designed, and its strength is enough to resist the applied load.

The test results of these specimens are shown in Table 4. These values agree well with the calculated values. The moment-rotation and moment ratio-plastic rotation diagrams for three SAC specimens are given in Fig. 14.

Since the beams of three SAC specimens have compact sections and strong material, the failure modes are of a rapid fracture type. The crack in the PN1 specimen initiated at the center of the bottom beam flange-column juncture. The crack rapidly propagated through the column flange and forked out into two cracks in the column

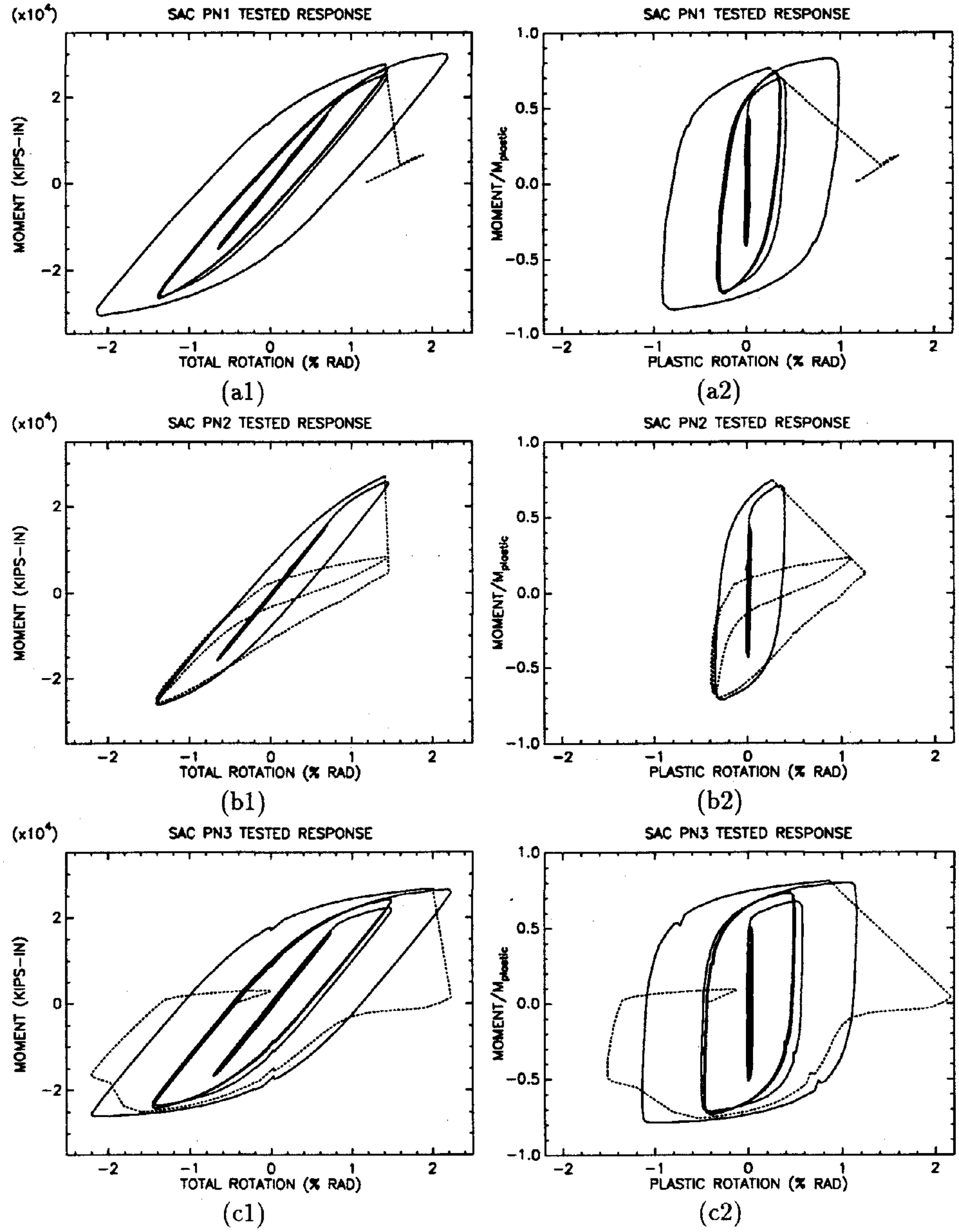

Fig. 14: Moment-rotation and moment ratio-plastic rotation diagrams for SAC PN1, PN2 and PN3 specimens.

Specimen Number	Load (kips)	Displacement Total (inches)	Displacement Beam (inches)	Post-yield cycles	Date & Temperature
PN1 - P_{yield}	154	1.31	1.15	$4\frac{1}{4}$	02/09/95
P_{peak}	225	2.91	2.63		60° F
PN2 - P_{yield}	153	1.34	1.11	$1\frac{1}{4}$	02/16/95
P_{peak}	201	1.94	1.71		50° F
PN3 - P_{yield}	138	1.12	1.02	$4\frac{1}{4}$	02/28/95
P_{peak}	199	3.02	2.88		60° F

Table 4: Test results of the SAC Joint Venture PN specimens.

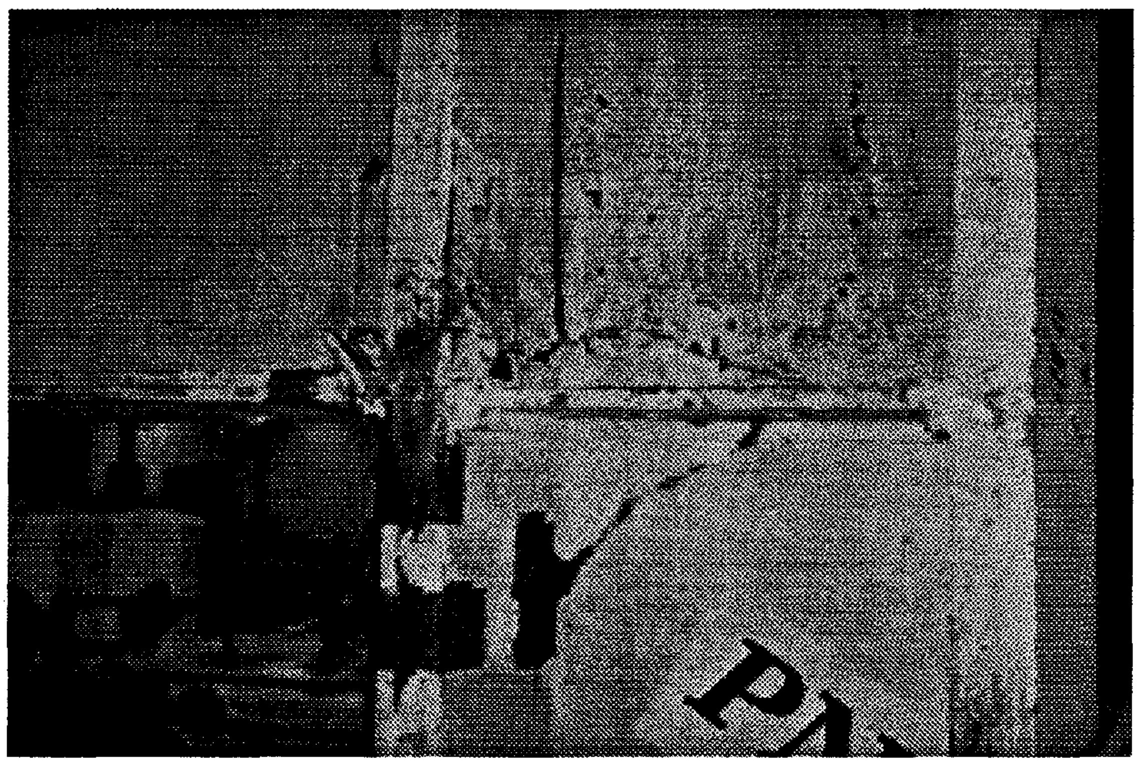

Fig. 15: Photograph of SAC specimen PN1 after test.

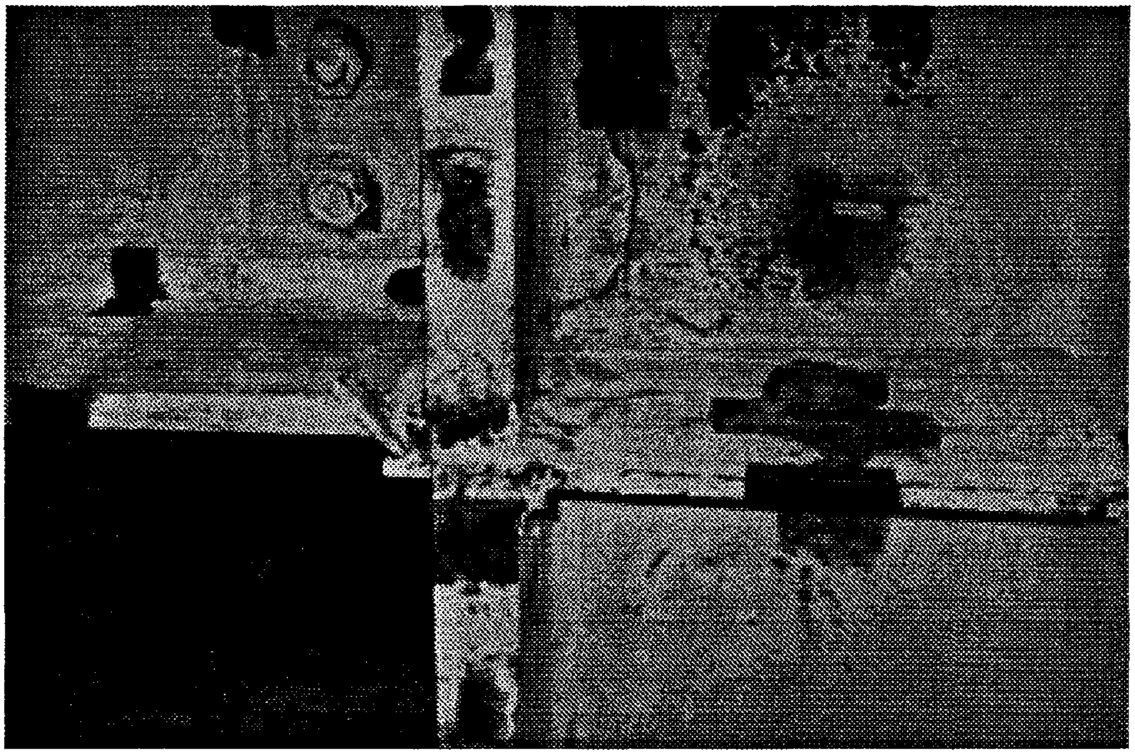

Fig. 16: Fracture pattern of SAC specimen PN2 is similar to specimen PN1.

web (see Fig. 15). At the peak load of 225 kips, the panel zone is unable to resist the applied shear force. The PN2 specimen has the same material properties as the PN1 specimen. Its fracture pattern is also similar to PN1 (see Fig. 16) except that the post-yield cycles are smaller. The peak load 201 kips is a little over the panel zone shear capacity. Specimen PN3 had a different fracture pattern compared with that of PN1 and PN2 specimens. The crack initiated at the center of the bottom beam flange-column juncture, then fractured the entire bottom beam flange (see Fig. 17). According to the classification in Table 2, PN1 and PN2 had failures of Type 2 because both had a strong beam and a relatively weak panel zone. The failure mode of PN3 is Type 1. All three specimens performed unsatisfactorily and failed in abrupt fractures. The imposed displacements and hysteresis loops for these specimens will be presented together with the analytical results in a later section.

It is interesting to note that if the beam of the SAC specimen had a yield strength of 36 ksi and an ultimate strength of 58 ksi, the performance of the connection would be much better and the failure mode would also be different. Compared with many successful connection tests back in the 1970s [22, 23], the design method and procedure are almost the same today. The most significant difference is that the

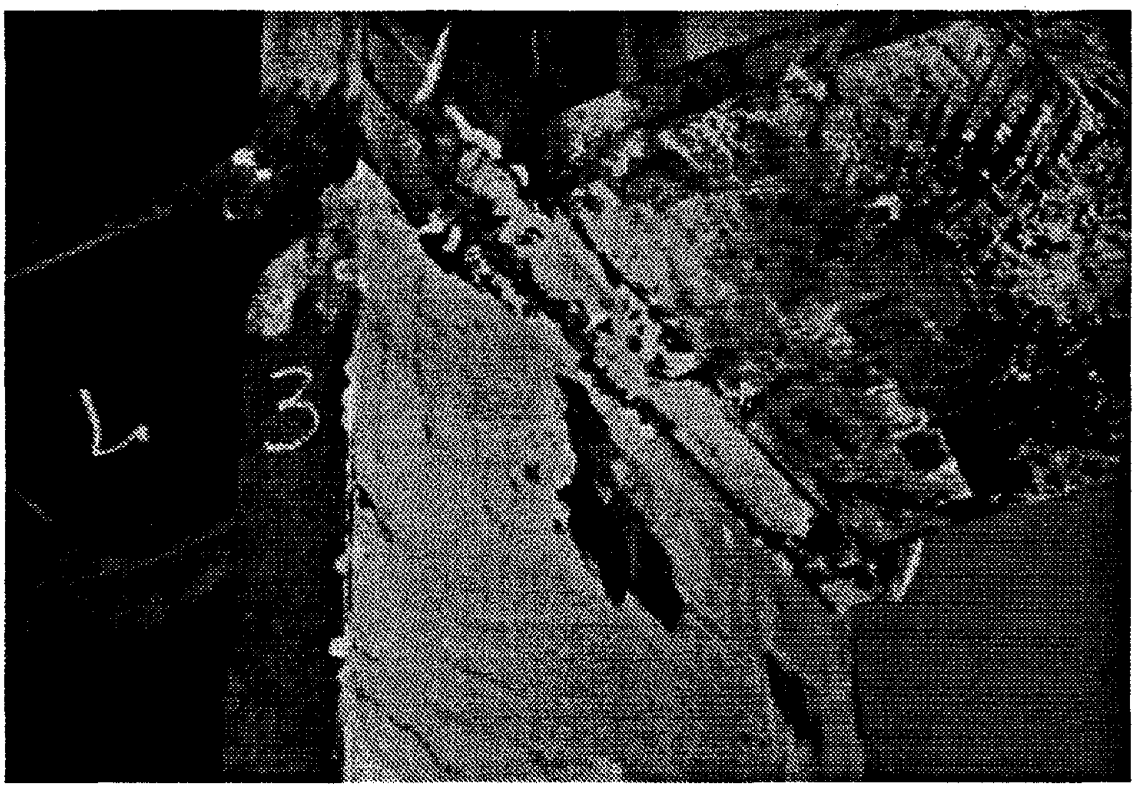

Fig. 17: Photograph showing the fractured bottom beam flange of SAC PN3 specimen after test.

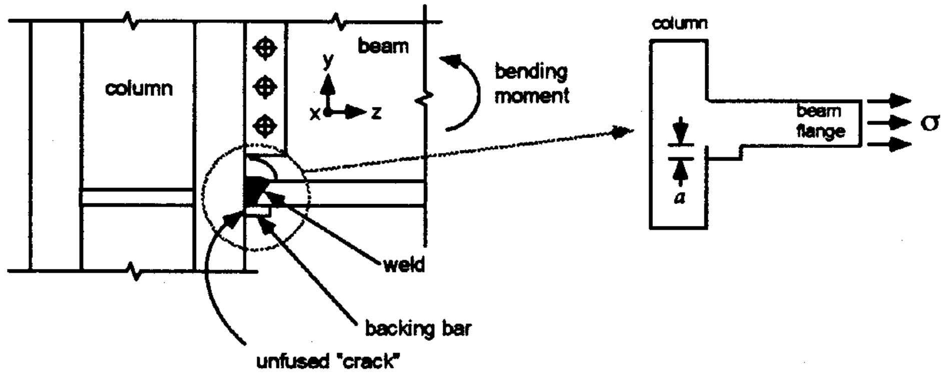

Fig. 18: The unfused backing bar surface forms an artificial edge crack.

material strength in the 1970s was much nearer to the ASTM specified minimum.

Stress Concentration Caused by the Backing Bar

If the backing bar has not been removed after the welding, the unfused interface between the backing bar and the column flange acts as a fine crack. The length of the crack is equal to the thickness of the backing bar (Fig. 18). Theories for analyzing the stress field near cracks are now well-established and can be found in many standard texts such as Anderson [2], Broek [9], Rolfe and Barsom [25], and Suresh [27]. The stresses in the vicinity of a crack tip in an elastic material can be expressed as [13, 14, 29]

$$\begin{aligned}
\sigma_{xx} &= \frac{K}{\sqrt{2\pi r}} \cos\left(\frac{\theta}{2}\right)\left[1 - \sin\left(\frac{\theta}{2}\right)\sin\left(\frac{3\theta}{2}\right)\right] \\
\sigma_{yy} &= \frac{K}{\sqrt{2\pi r}} \cos\left(\frac{\theta}{2}\right)\left[1 + \sin\left(\frac{\theta}{2}\right)\sin\left(\frac{3\theta}{2}\right)\right] \\
\sigma_{xy} &= \frac{K}{\sqrt{2\pi r}} \cos\left(\frac{\theta}{2}\right)\sin\left(\frac{\theta}{2}\right)\cos\left(\frac{3\theta}{2}\right)
\end{aligned} \tag{27}$$

for a crack aligned in the x direction, where K is the stress intensity factor, r, θ are the cylindrical polar coordinates of a point with respect to the crack tip. Thus each case is characterized by the stress intensity factor having a spatial distribution of stresses. One of the underlying principles of fracture mechanics is that unstable fracture occurs when the stress-intensity factor K at the crack tip reaches a critical value K_c. To prevent a fracture failure, the computed stress-intensity factor K must be less than the critical stress-intensity factor, or fracture toughness, K_c.

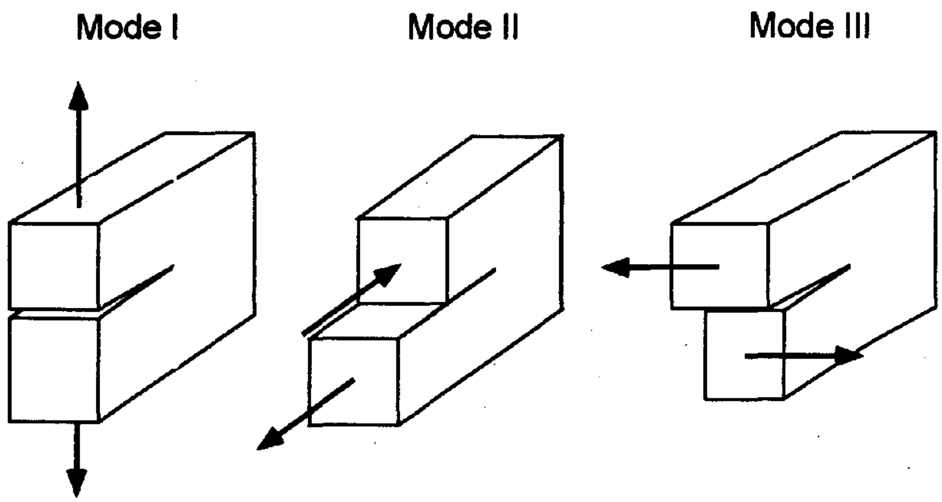

Fig. 19: The three modes of loading that can be applied to a crack: Mode-I (Opening), Mode-II (In-plane shear), and Mode-III (Out-of-plane shear).

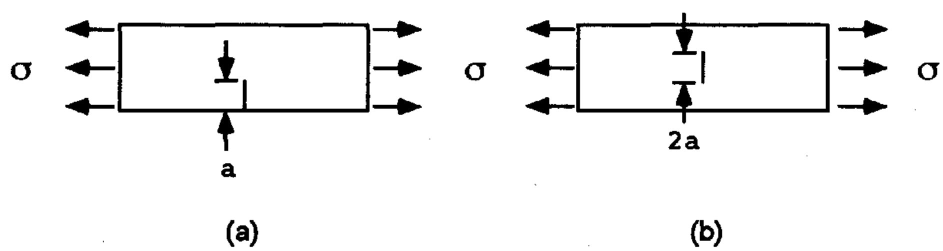

Fig. 20: A semi-infinite plate with (a) edge crack, (b) center crack subject to a remote axial stress σ.

The "artificial crack" between the unfused backing bar and the column flange can be characterized as an edge crack. There are three possible fracture modes of a crack (Fig. 19), namely Mode-I (Opening), Mode-II (In-plane shear), and Mode-III (Out-of-plane shear). Tension in a beam flange due to bending opens the crack in mode-I[3]. The Mode-I stress-intensity factor for the edge crack is shown to be

$$K_I = 1.12\sigma\sqrt{\pi a} \tag{28}$$

where a is the crack length, here the thickness of the backing bar, and σ is the applied nominal Mode-I stress (Fig. 20(a)). The critical stress-intensity factor K_{Ic} of Mode-I

[3]The shear and torsional forces in the beam can also open the crack in mode-II and mode-III, respectively, but their magnitudes are relatively small and can be ignored.

can be obtained by following the ASTM standard for determining K_{Ic} [3]. K_{Ic} is temperature sensitive. For carbon steel, the transition is quite steep at temperatures above 0°F.

K_{Ic} can also be obtained from the critical energy release rate $\mathcal{G}$ (after Griffith [11]) of the material from

$$K_{Ic} = \sqrt{\mathcal{G}E'} \tag{29}$$

where E' is the modified modulus of elasticity, it can be computed as

$$E' = \begin{cases} E & \text{for plane stress} \\ E/(1-\nu^2) & \text{for plane strain} \end{cases} \tag{30}$$

where E is the Young's modulus and ν the Poisson's ratio. The crack between the backing bar and column flange is long enough to be considered as a plane strain problem.

The critical energy release rate $\mathcal{G}$ is temperature sensitive. For structural carbon steel, it is known that $\mathcal{G}$ is at least 15 lb-ft (see [4, 26]). The critical stress-intensity factor can be calculated to be

$$K_{Ic} = 75.7 \text{ ksi}\sqrt{\text{in}} \tag{31}$$

Based on this value and in the case that $K_I = K_{Ic}$, if the thickness of the backing bar is 3/8 inch, then the nominal stress $\sigma_{zz} = \sigma$ in the beam flange, according to Eq. 28, cannot be more than 62 ksi.

There are two ways to reduce the deleterious effect of the backing bar. A direct method is to remove it using a carbon arc. Once the backing bar has been removed, the artificial crack no longer exists. But this method has a high probability of damaging a good weld above the backing bar. Another method to reduce the stress concentration caused by the backing bar is to apply a fillet weld under it to close the crack. A center crack of length $2a$ occurring away from the edges, such as the one shown in Fig. 20(b), has a somewhat smaller stress-intensity factor, namely,

$$K_I = \sigma\sqrt{\pi a} \tag{32}$$

Here, a is half of the backing bar thickness. Therefore, an additional fillet weld under the backing bar will reduce the stress-intensity factor and improve the connection fracture resisting capability.

In this section, it is assumed that the stress σ across the beam flange is uniform with linear elastic behavior, but in reality, σ is not uniform. The geometry of the backing bar crack is not similar to the edge or center crack shown in Fig. 20. Applying Eqs. (28) and (32) to the backing bar crack problem is oversimplified. To account for the effects of the geometry, non-uniform stress distribution, and elastic-plastic material behavior, the numerical J contour integration by finite element method must be used.

Nonlinear Finite Element Analysis

In order to accurately evaluate the stress distribution and the stress-intensity factor at the connection, the SAC specimens are modeled on eight-node brick elements in the ABAQUS finite element package [12]. The element mesh of the connection part of the specimen is shown in Fig. 21. Note that the backing bars together with the artificial cracks mentioned previously are introduced in the model. As of this writing, the SAC specimens are being retrofitted for re-testing, and no tension tests for the material are available at the moment. Because the true material properties are unknown, the material properties used in the finite element model are based on the Mill Certificates as given in Table 3. The coupon test will be scheduled right after the completion of structural testing of the retrofitted connections. The material properties were modeled by von Mises yield criterion with associated plastic flow.

To fully understand the stress distribution and propagation during the structural testing, the same imposed beam tip displacements were used in the finite element computations. Because the applied loads are slowly varying in the test, the inertia loads are ignored in the finite element analysis. Figure 22 displays the imposed tip displacements for experimental and analytical studies of the PN1 specimen. The analysis steps shown in the figure are not evenly spaced because it requires more steps in the nonlinear region. To accelerate the analysis, low amplitude displacement cycles are ignored in the analysis, these including two 0.1 in. cycles, three 0.25 in. cycles, and three 0.5 in. cycles. Because the hot rolling residual stresses and the heat-affected zone residual stresses are not fully known, such effects are also ignored in analyses. Such simplification make the corners in the analytical hysteresis loops sharper than the experimental ones. The experimental and analytical hysteresis loops for the SAC PN1 Specimen are presented in Fig. 23. The experimental and analytical imposed displacements and hysteresis loops for the SAC PN3 specimen are shown in Figs. 24 and 25, respectively. The low amplitude displacement cycles are also ignored in the PN3 analysis. By integrating the hysteresis loops step-by-step, the total energy

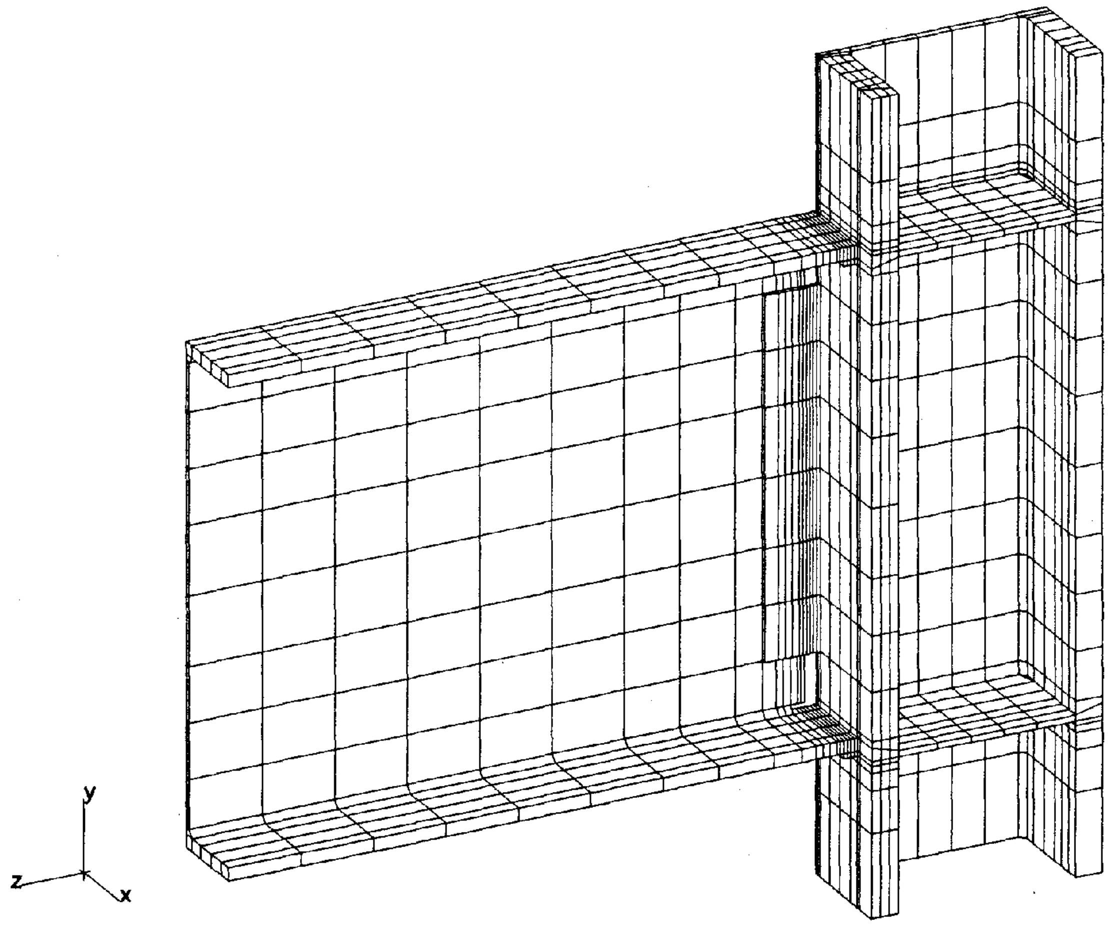

Fig. 21: Finite element mesh for SAC Pre-Northridge PN connection. Only one half of the specimen is modeled.

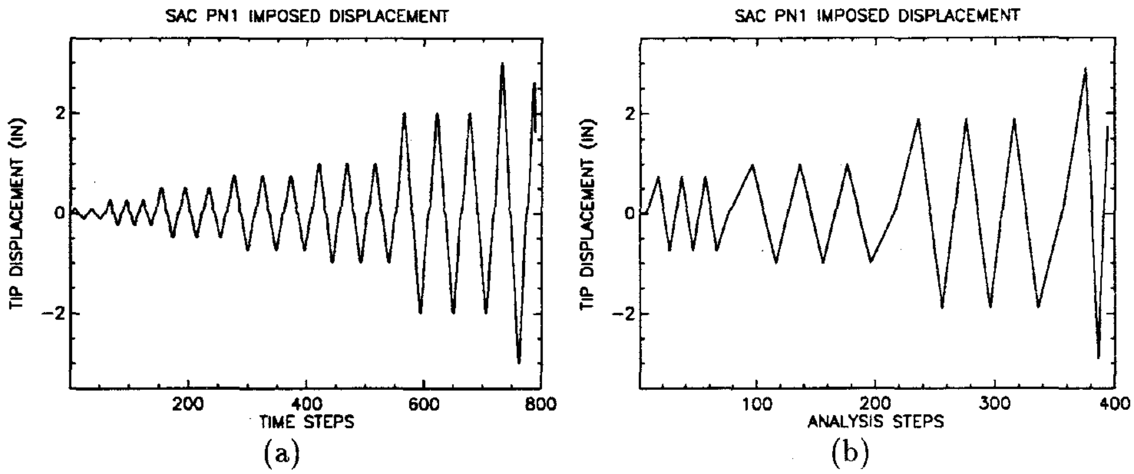

Fig. 22: (a) Imposed tip displacements used in testing SAC PN1 specimen, and (b) imposed tip displacements used in finite element analysis.

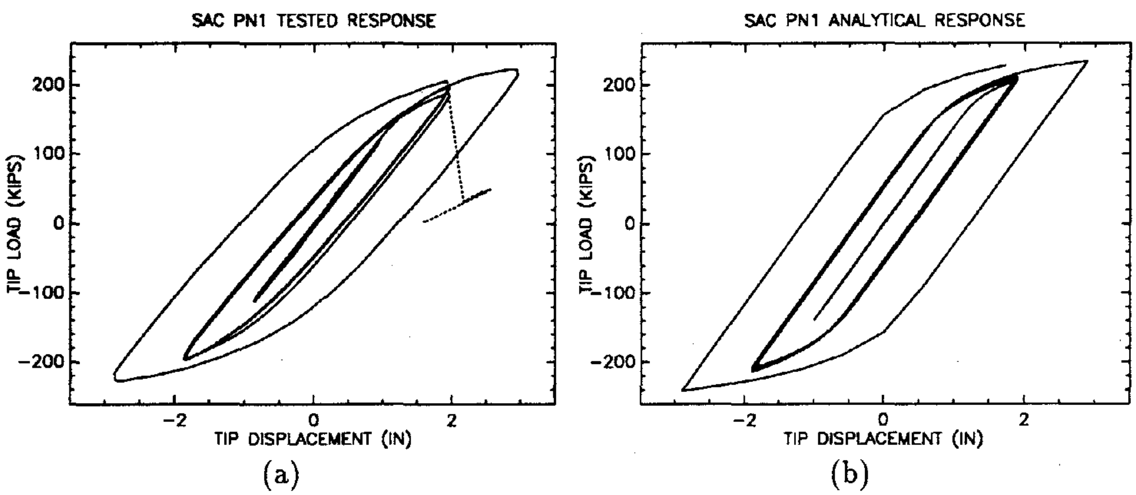

Fig. 23: (a) Experimental and (b) analytical hysteresis loops of SAC PN1 specimen (Displacements are measured in the loading direction).

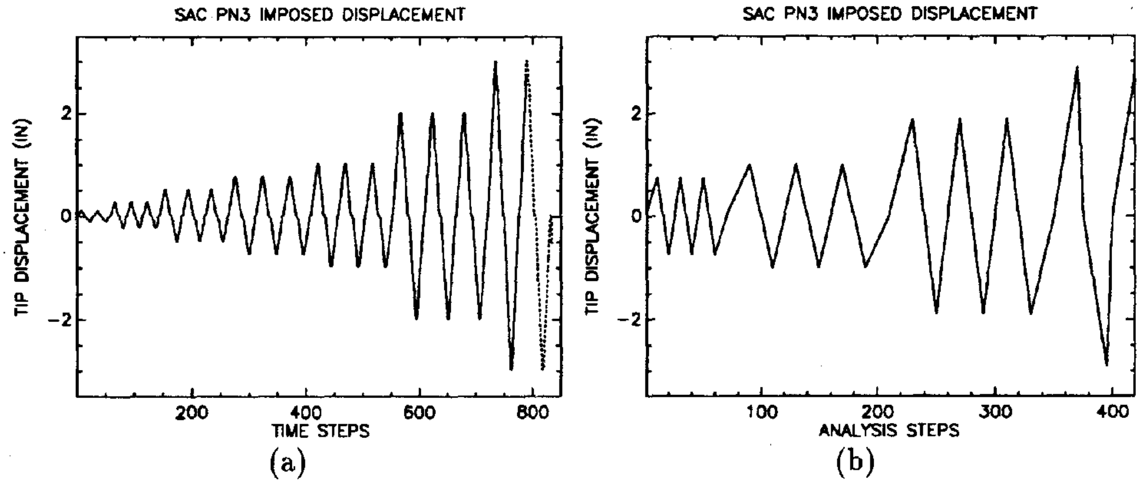

Fig. 24: (a) Imposed tip displacements used in testing SAC PN3 specimen, and (b) imposed tip displacements used in finite element analysis. The dashed line represents the imposed displacements after the bottom beam flange was fractured.

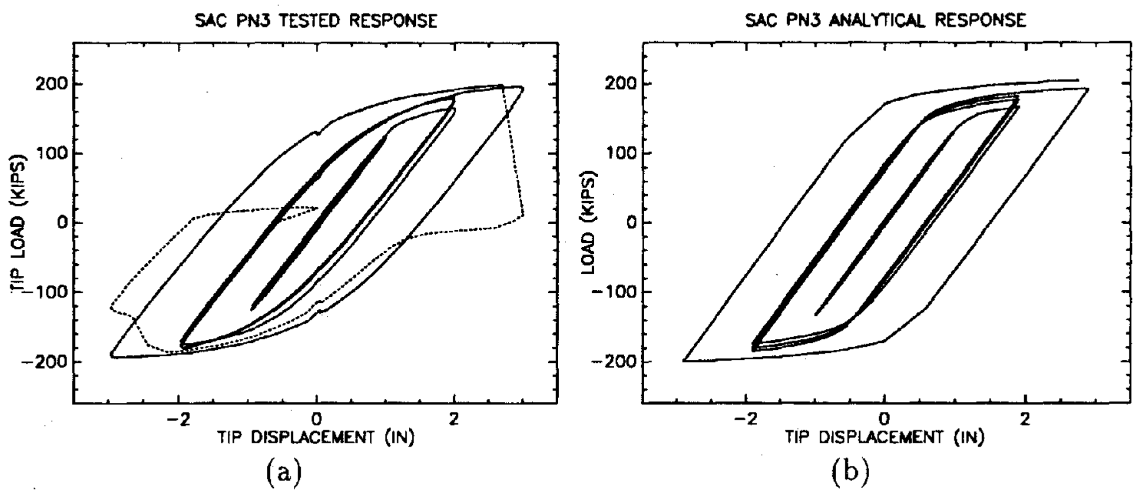

Fig. 25: (a) Experimental and (b) analytical hysteresis loops of SAC PN3 specimen (Displacements are measured in the loading direction). The dashed curve represents the response after the fracture of the bottom beam flange.

diagram can be constructed. The total strain energies of PN1 and PN2 specimens are given in Fig. 26. The wavy shape curve in the total energy diagram is due to the restoration of elastic strain energy during load reversals. Those unrecoverable energies are dissipated energy. The same diagrams for the PN3 specimen are given in Fig. 27. These figures lead to the conclusion that none of the three SAC specimens possessed adequate energy dissipating capacities.

Among the three SAC specimens, PN2 has the least ductile behavior. The imposed displacements and load-deflection responses are shown in Fig. 28. Because the PN2 specimen is identical to the PN1 specimen, the analytical response of the PN1 specimen can be used for comparison. The total energy diagram for the PN2 specimen is given in Fig. 26(a).

A perspective view of the connection stress distribution is shown in Fig. 29. The highest stressed spots are at the beam flange weld and in the panel zone. The material yielding in the panel zone starts at the center and then gradually expands outward. During the test, the whitewash was continuously breaking off in the panel zone. When the tip load reached about 200 kips, the entire panel zone yielded. The analytical stress contours in Fig. 30 agree with this observation. Figures 31 and 32, respectively, show views of the stress contours of the top and bottom beam flanges, together with the continuity plates and column section in the plastic range. In the elastic range, the largest stress occurs at the center of beam flange-column juncture. The stresses become much more evenly distributed across the beam flange in the plastic range, but the center of the flange still has the largest stress. All the displacements in these figures are magnified 10 times. Even so, there is no obvious deformation observed in the axial direction of the beam flange.

The SAC PN1/PN2 stress distributions for the bottom beam flange along the line of groove weld are shown in Fig. 33. Curves shown are for beam tip loads of 21, 41, 62, 82, 103, 117, 142, 200, and 225 kips. Shearing stresses are not shown because their values are small. The maximum shearing stresses at 225 kips tip load are 3.6 ksi, -17.4 ksi, 17.5 ksi for σ_{xy}, σ_{xz}, and σ_{yz}, respectively. Small shearing stresses imply small shearing deformations and small ductility of the connection.

The experimental strains at the center of the panel zone are plotted against the applied tip load for three SAC specimens (see Fig. 34). The load-shear strain diagrams show large shear strain in the PN1 panel zone, but much smaller shear strain in the PN2 and PN3 panel zones. The PN3 panel zone resists smaller shear force, its panel zone shows only slight yielding but no fracture. From the material strength point of

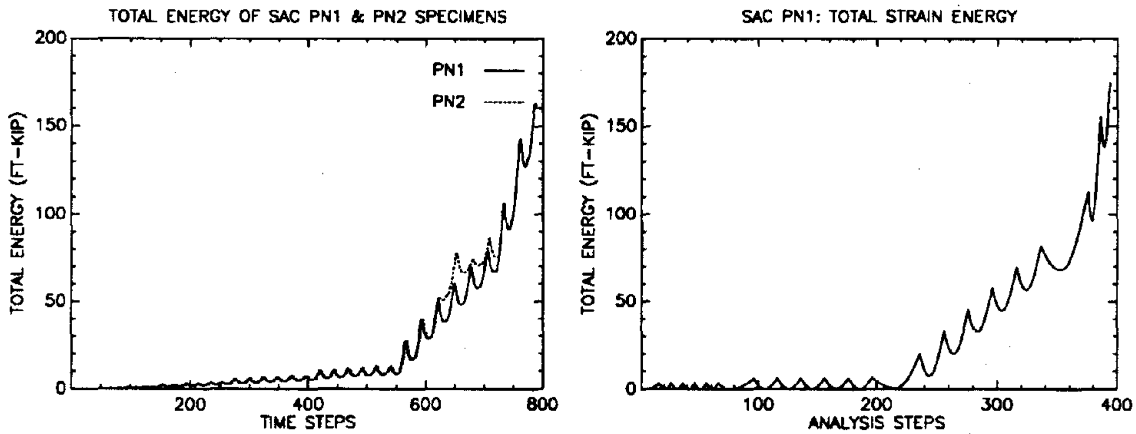

(a) (b)

Fig. 26: (a) Experimental and (b) analytical total strain energy diagrams of SAC PN1 and PN2 specimens.

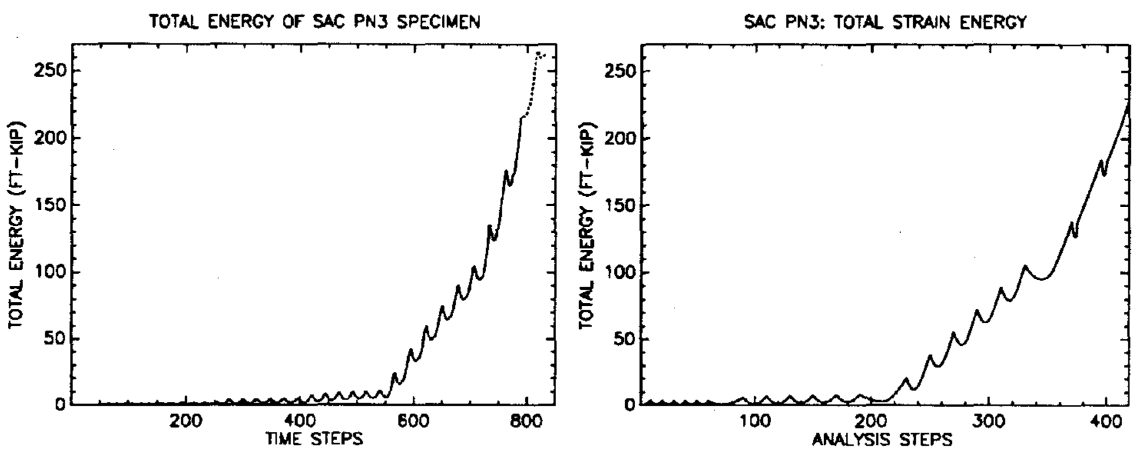

(a) (b)

Fig. 27: (a) Experimental and (b) analytical total strain energy diagrams of SAC PN3 specimen.

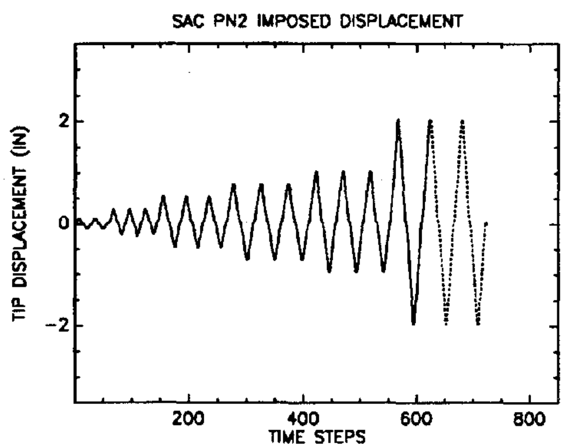

(a)

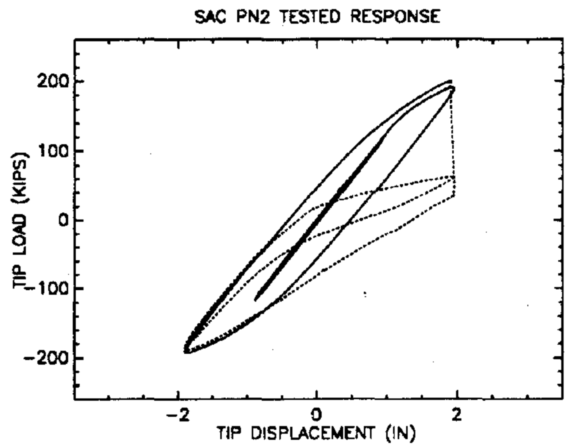

(b)

Fig. 28: (a) Imposed displacements and (b) hysteresis loops of SAC PN2 specimen (Displacements are measured in the loading direction). The dashed curves represent the response after the fracture of the bottom beam-column juncture.

view, there is no doubt that PN1 failed in the panel zone by overstressing, but it is difficult to reach the same conclusion for PN2, although both have the same fracture pattern in the panel zone. It is much simpler to explain this by fracture mechanics.

The J contour integrals along the top and the bottom backing bar crack tip are evaluated. In calculating the J contour integral using the finite element method, the nonlinear elastic-plastic material properties are considered. Rice had formulated the J contour integral defined to be [24]

$$J = \int_{\Gamma} \left(w dy - T_i \frac{du_i}{dx} ds \right) \tag{33}$$

for a crack aligned in the x direction. Here, Γ is any contour from the lower crack face counterclockwise around the crack tip to the upper face. The path length along this contour is s, w is the strain energy density defined as

$$w = \int_0^{\epsilon_{ij}} \sigma_{ij} d\epsilon_{ij} \tag{34}$$

where σ_{ij} and ϵ_{ij} are the stress and strain tensors, respectively. $T_i u_i$ are work terms for components of surface traction on the contour path, T_i, move through displacements, du_i. The J contour integral is equal to the energy release rate for a linear or nonlinear elastic material under quasi-static conditions. The integral was shown to be independent of choice of path for a crack with stress-free faces. Since the critical value J_c for A572 Grade 50 is unavailable, it is impossible to justify the initiation of fracture

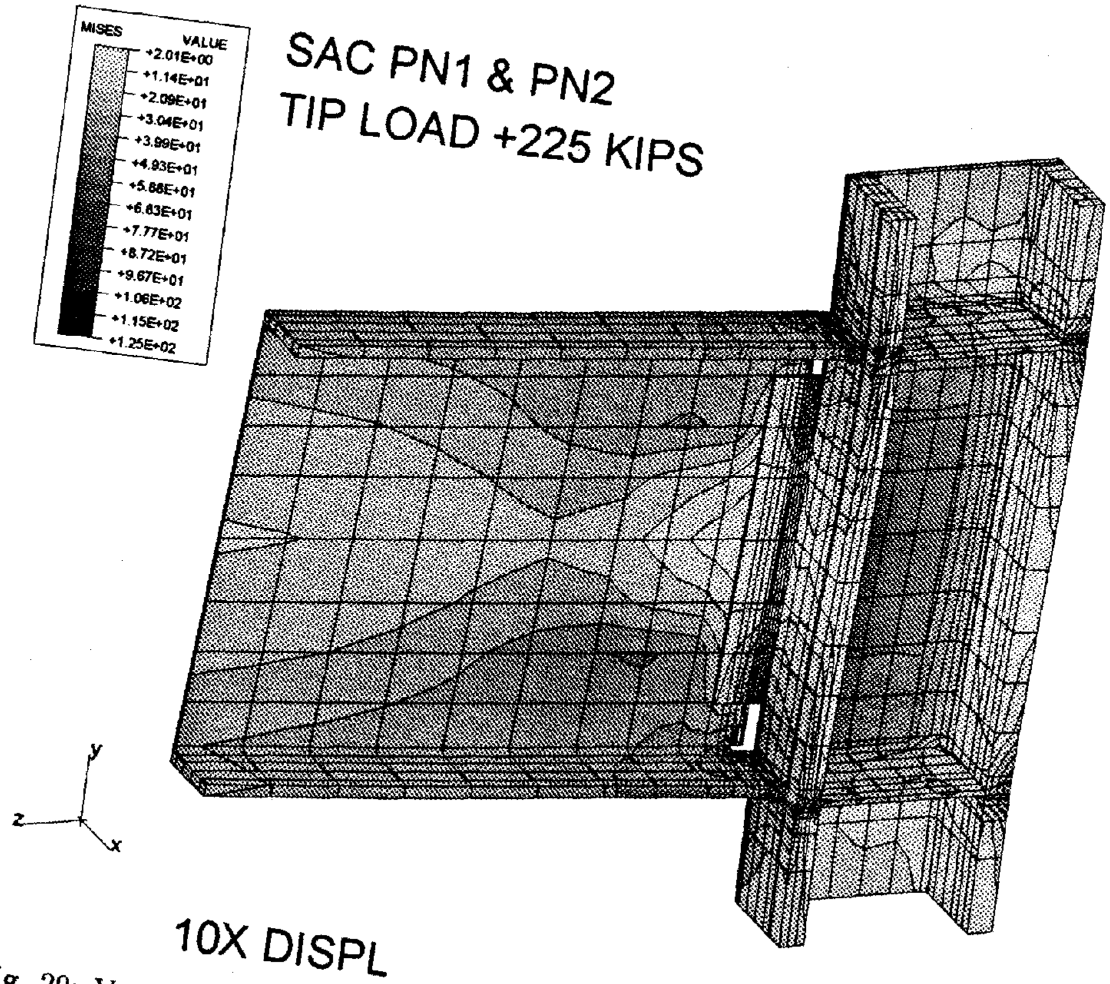

Fig. 29: Von Mises Stress contours for SAC PN1/PN2 under 225 kips tip load.

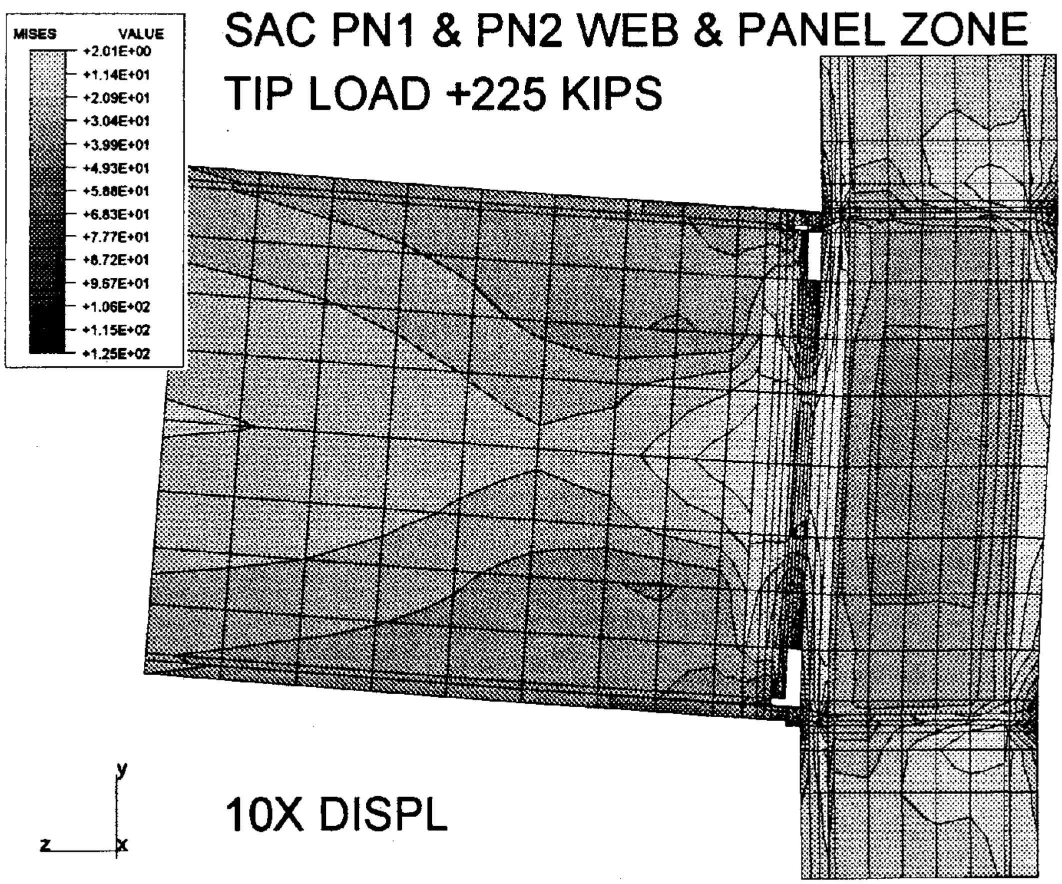

Fig. 30: Web and panel zone stress contours for SAC PN1/PN2 under 225 kips tip load.

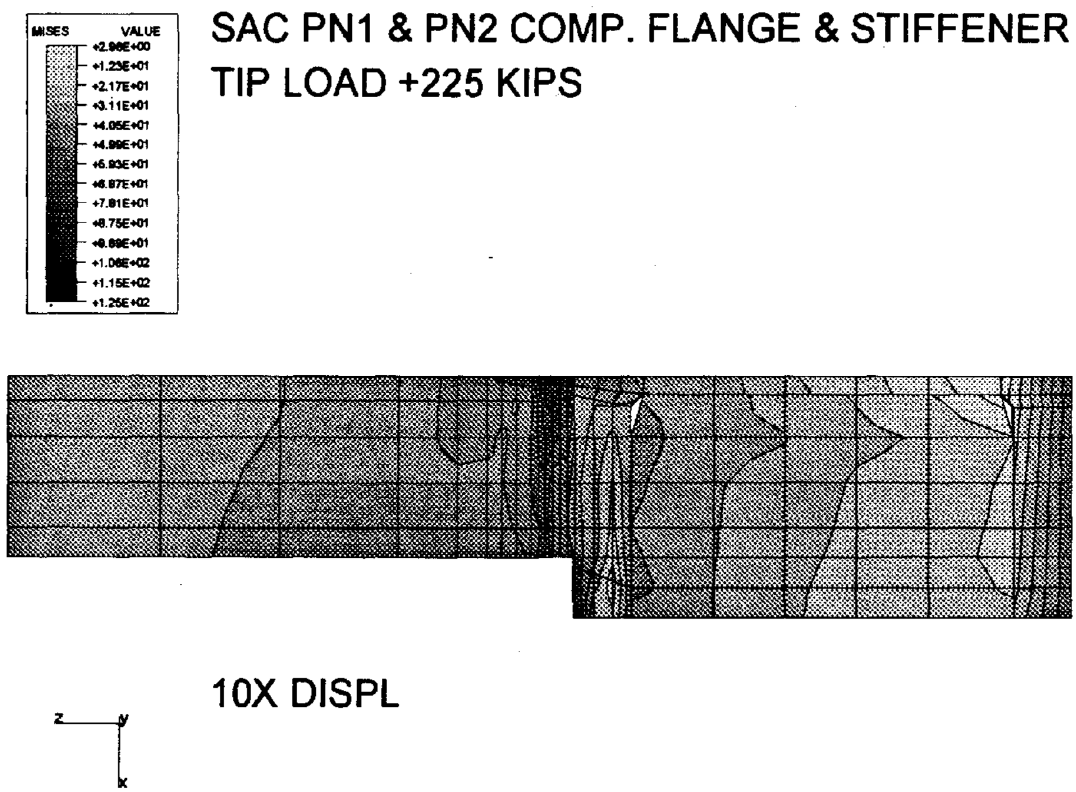

Fig. 31: Top beam flange and continuity plate contours for SAC PN1/PN2 under 225 kips tip load.

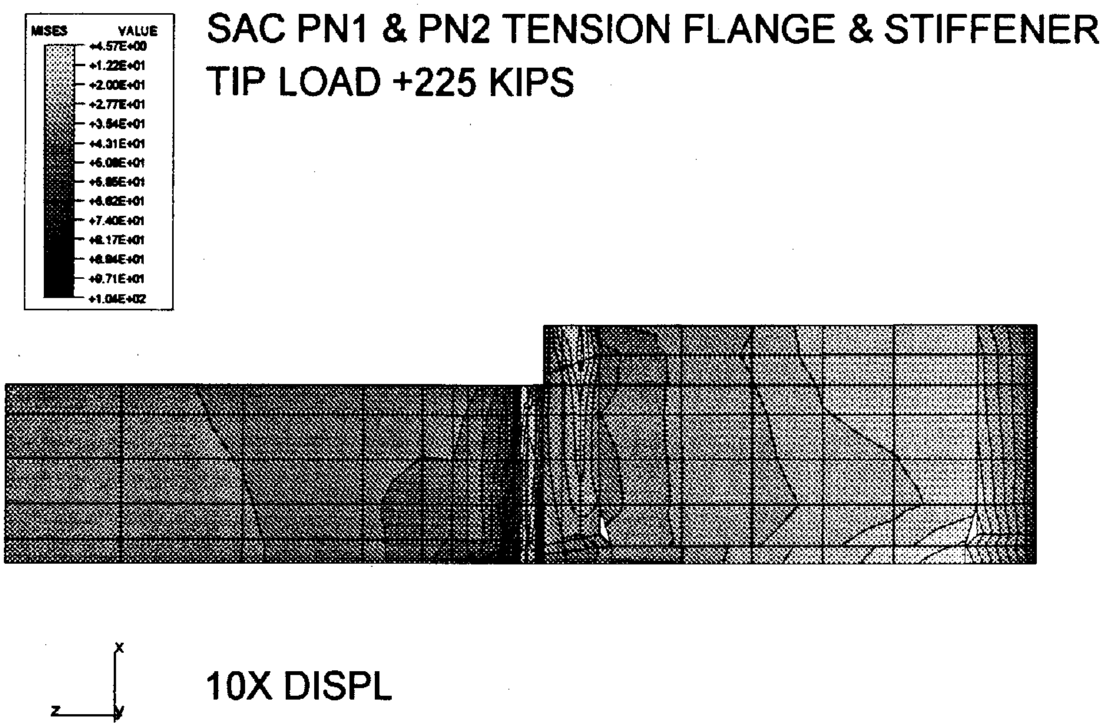

Fig. 32: Bottom beam flange and continuity plate contours for SAC PN1/PN2 under 225 kips tip load.

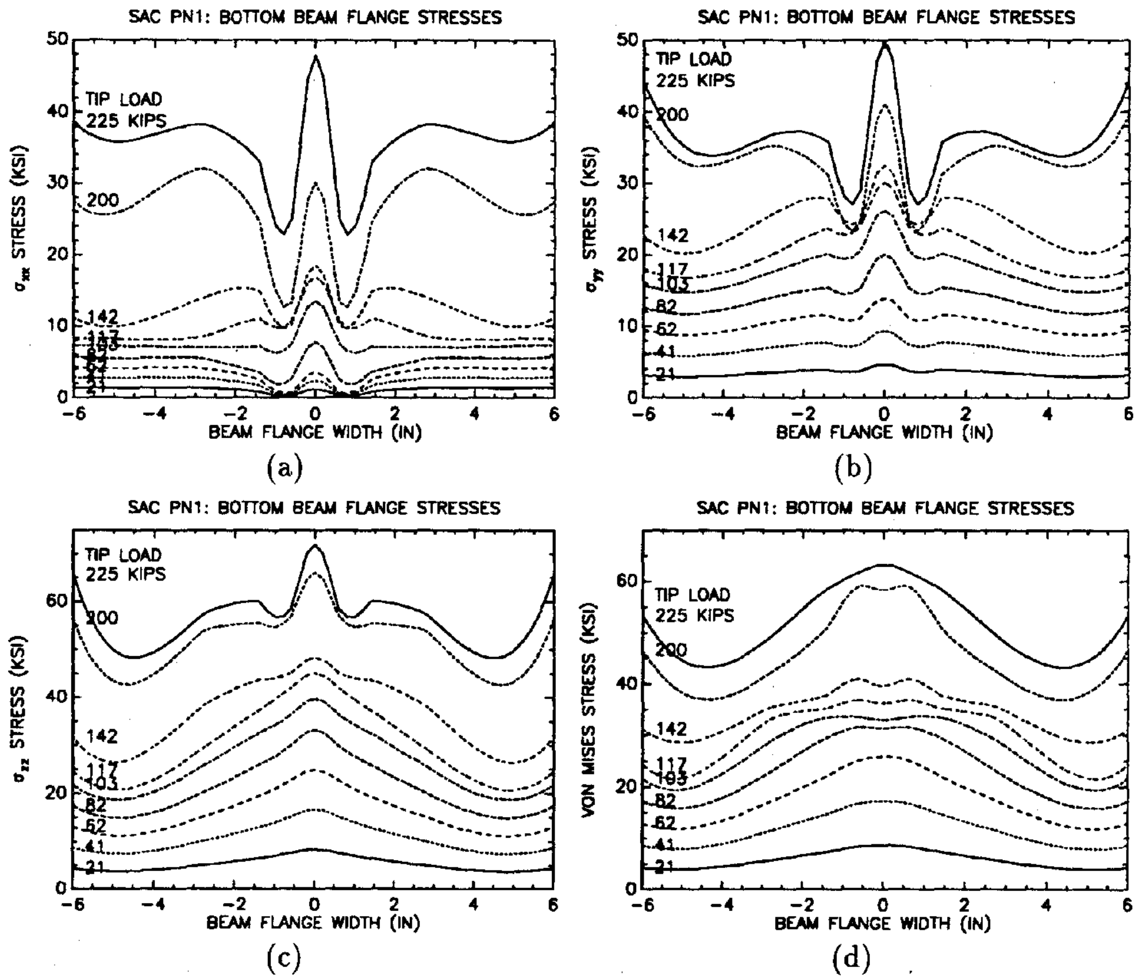

Fig. 33: Stress distribution across the bottom beam flange at weld for SAC PN1 and PN2 specimens: (a) σ_{xx}, (b) σ_{yy}, (c) σ_{zz}, and (d) von Mises stress.

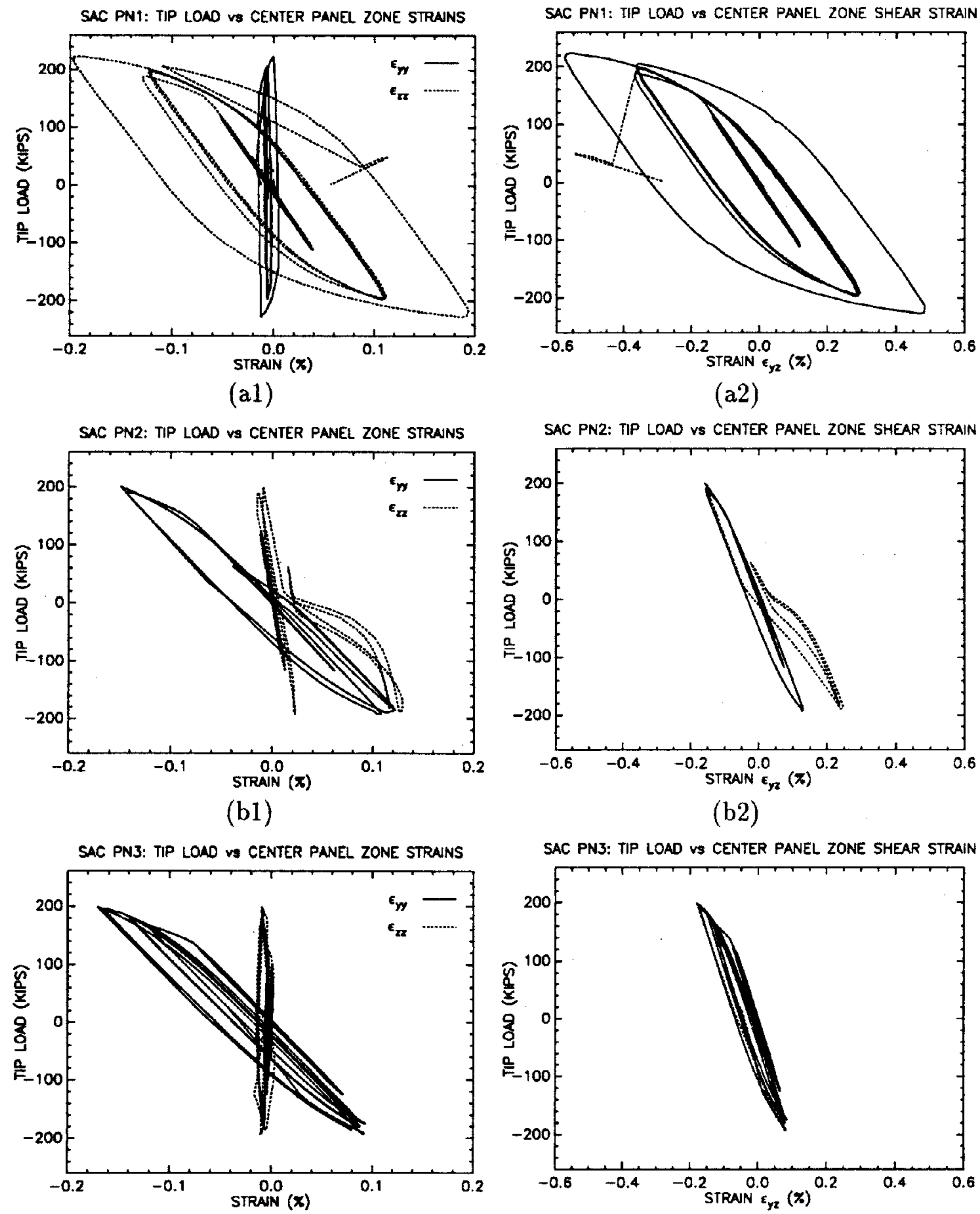

Fig. 34: Center panel zone strains vs tip load for SAC PN1, PN2 and PN3 specimens.

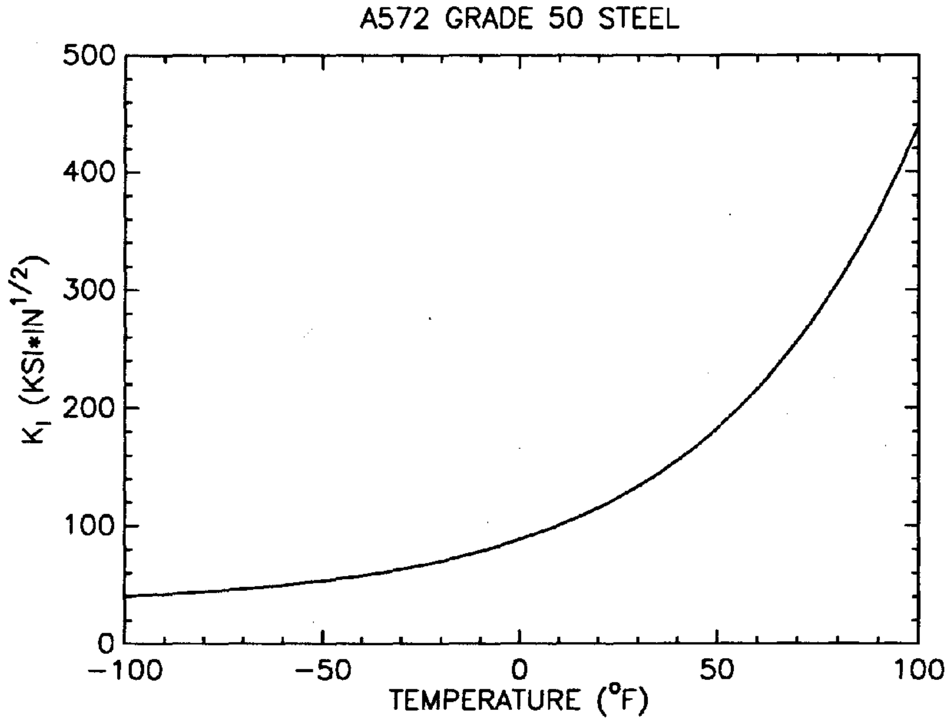

Fig. 35: Stress intensity factors plotted against temperatures obtained from 1.5-in.-thick plates of A572 steel.

based on the computed J values. Fortunately, the specific temperature induced variation in stress intensity factors for the 1.5-in.-thick A572 Grade 50 specimens tested is available and presented in Fig. 35 [20]. In order to compare the calculated J values with the known K_{Ic}, an equivalent K_I is calculated [15]:

$$\frac{K_I^2}{E'} = J \tag{35}$$

where E' is defined in Eq. (30). It is thus conceptually equal to the Griffith term $\mathcal{G}$. Strictly speaking, the above equation only holds under elastic conditions. But if the plastic zone at the crack front is small, this equation is valid. The equivalent K_I values from the computed J values for the top and the bottom backing bar for PN1 and PN2 are shown in Fig. 36. In the figures, K_I values are plotted against beam width and analysis steps. It can be seen that the largest K_I occurs at the center of the beam flange-backing bar juncture. If the connection fractures, it will start at the point with the largest stress intensity factor. It is interesting to re-plot the largest stress intensity factor vs. the applied tip load (see Fig. 37). The growth of K_I due to cyclic load can be seen. The critical stress intensity factors at 0°F, 50°F and 60°F taken from Fig. 35 are also plotted in the diagram. The most interesting finding in

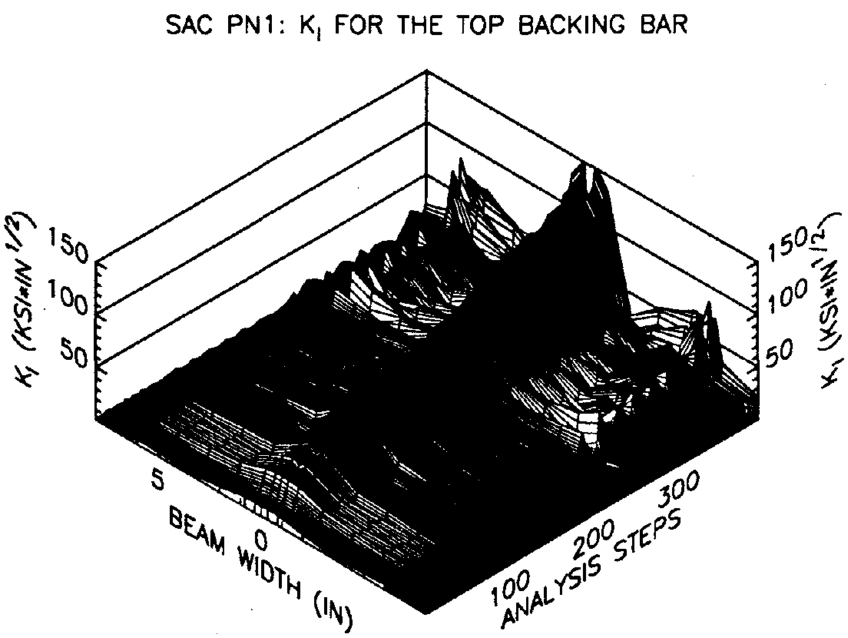

(a)

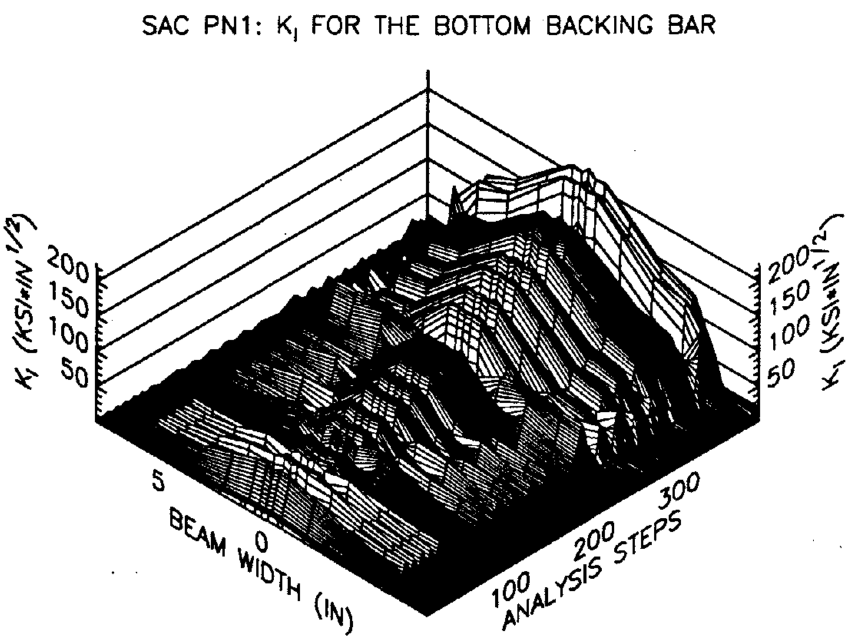

(b)

Fig. 36: Stress-intensity factors plotted across beam width and number of analysis steps at (a) top and (b) bottom backing bars for SAC PN1 and PN2 specimens.

the figure is that the bottom backing bar K_I at a given time is larger than that of the top backing bar. This clearly explains why most of the connection fractures during the Northridge earthquake initiated at the bottom backing bar.

It is also interesting to re-plot the largest K_I vs. tip displacement (see Fig. 38). It can be seen that the stress intensity factor keeps on growing under the same-amplitude cycles, elastic or inelastic; the larger the displacement amplitude, the larger the K_I growth rate. When K_I grows over the K_{Ic}, the connection will fracture. Based on the K_I growth rate, it is easy to predict the low-cycle fatigue fracture of the connection. The effect of temperature can be seen in these plots; the higher the temperature, the larger the K_{Ic}, and the less likely is the connection to fracture. The SAC PN1 and PN2 specimens are theoretically identical, but the PN1 specimen sustains more cycles of loading than PN2. One of the reasons to explain this is the different temperature. PN2 was tested on a cooler day. The low K_{Ic} value at the lower temperature meant PN2 fractured earlier.

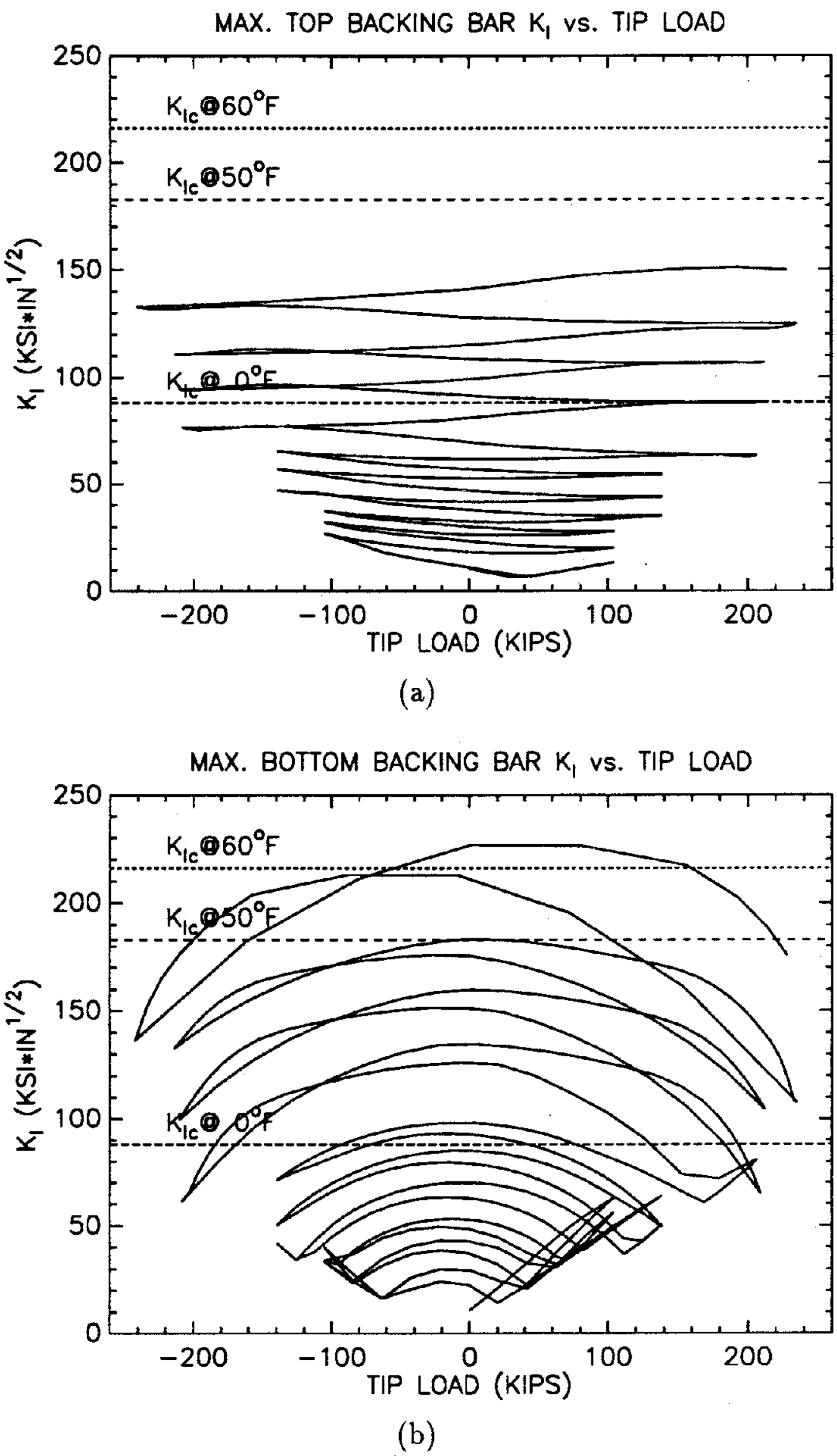

Fig. 37: Maximum stress-intensity factors vs. tip load at (a) top and (b) bottom backing bars for SAC PN1 and PN2 specimens.

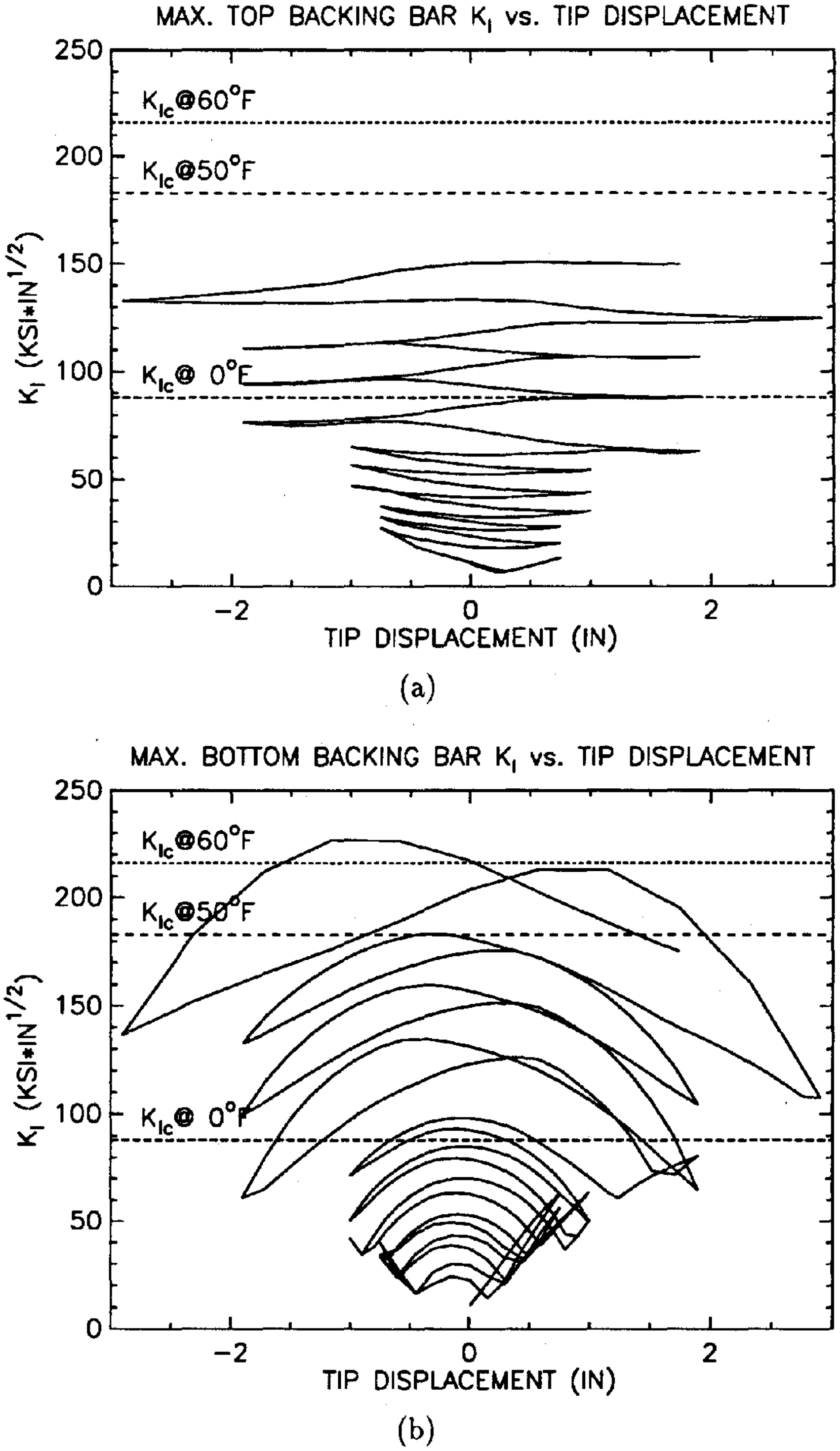

Fig. 38: Maximum stress-intensity factor vs. tip displacement at (a) top and (b) bottom backing bars for SAC PN1 and PN2 specimens.

Conclusion

On the basis of these limited analytical and experimental studies, the following conclusions can be drawn:

1. Elementary mechanics calculations can predict the connection capacity very well as long as the material properties are known in advance.

2. The connection made by directly welding a compact beam flange to a column cannot attain the plastic moment of the beam. To protect the connection from failure, a weaker beam should be used or reinforcement of the connection should be made. A weaker beam means a beam with a non-compact section such that the local buckling moment is smaller than the connection moment capacity. If a compact beam must be used, the beam can be made weaker by drilling holes in the flange near the connection so that the moment transferred to the connection is smaller (Fig. 39). There are several ways to reinforce the connection; one of the methods is by using flange cover plates with thickness greater than the beam flange thickness. But such connection requires two welds, a weld to the beam and a weld to the column, which increases the cost substantially.

3. The elastic stress concentration factor at the beam flange of the welded beam-to-column connection can range between 1.2 to 1.46. The stresses will redistribute much more evenly across the flange when loaded into the plastic range. The largest stress is located at the center of the welded flange.

4. Triaxial loading makes steel at a connection fail without exhibiting yielding ductile behavior. This is due to the state of stress and not because of the material property. The demand for ductility should be dependent on the material yielding near the connection area.

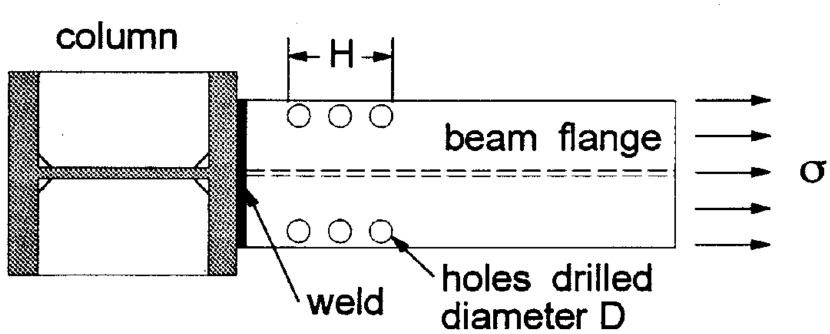

Fig. 39: Connection protection by beam flange perforation.

5. Material properties of steel, such as yield strength and ultimate strength, should be regulated to have a narrow range instead of prescribing only the minimum strength. Otherwise, an engineer cannot design a structure with tolerable bounds on response. Today's A36 steel has an average yield strength 33% over the minimum. This fact is not reflected in present design codes nor in education. This high strength does not enable the connection to develop a plastic hinge during a strong earthquake and causes its failure in brittle fracture.

6. The column web fracture is due to a weak panel zone. Using doubler plate in the panel zone may solve the problem, but will increase the construction cost. The best solution is to avoid connecting a strong beam to a column with weak web. Connecting a beam to the minor axis of a column allows for the use of column flanges to resist the shear.

7. The dimensions of many rolled shapes should be made to better proportions. For example, the W14×257 section used in the SAC specimens has a large moment capacity but a very small capacity in shear resistance.

8. The unfused surface between the backing bar and the column can be characterized as an edge crack. If the backing bar cannot be removed, an extra fillet weld under the backing bar can close the crack and makes the stress-intensity factor smaller, and thus safer. During load reversals, the stress intensity factor at the bottom backing bar crack is higher than that at the top backing bar, resulting in greater probability of initial fracture at the bottom weld during an earthquake.

9. Welded connections exposed to outside temperatures should be designed very carefully because steel has a lower critical stress-intensity factor at low temperatures. This is especially true for connections with backing bars and welding flaws.

10. Energy dissipation at a connection by the means of material yielding is notoriously unreliable. A small variation from the design value in beam or column strength will easily result in a totally different energy dissipating mechanism and failure mode.

The following important issues were not considered in this limited study, and require further research:

1. Finite element analyses need to be re-done using the true material properties after the completion of the coupon test of the SAC PN specimens. High-order singularity elements should be used in modeling the crack for higher accuracy.

2. The residual stress distribution at the heat affected zone of a weld requires further investigation.

3. The internal flaw sizes between multiple layers of weld must be investigated, especially, since the crack growth due to cyclic yield loads induces low cycles fatigue fracture. Such a problem will stand out in a long duration earthquake.

4. The databases of fracture toughness of structural steel and welding materials in the plastic range need to be established.

5. J contour integration analysis for the backing bar with additional under bar fillet weld is useful in understanding its merit quantitatively.

6. The welded connection, unlike the bolted connection, lacks crack resisting redundancy. Further investigation of the crack arresting design is required.

References

[1] Alpsten, G. A., *Thermal Residual Stresses in Hot-Rolled Steel Members*, Fritz Laboratory Report 337.3, Lehigh University, 1968.

[2] Anderson, T. L., *Fracture Mechanics, Fundamentals and Applications,* 2nd ed., CRC Press, 1995.

[3] ASTM, *Standard Test Method for Plane-Strain Fracture Toughness of Metallic Materials.* E399-90, American Society for Testing and Materials, Philadelphia, 1990.

[4] Barsom, J. M.,"Development of the AASHTO Fracture Toughness Requirements for Bridge Steels," *Engineering Fracture Mechanics,* **7**, 605-618, 1975.

[5] Beedle, L. S. and Tall, L., "Basic Column Strength," *Proc. Am. Soc. Civil Engrs.*, **86** (ST-7), 139, July 1960.

[6] Bertero, V. V., Anderson, J. C., and Krawinkler, H., "Performance of Steel Building Structures During the Northridge Earthquake," *Report No. UCB/EERC-94/09*, Earthquake Engineering Research Center, University of California, Berkeley, 1994.

[7] Blackman, B., *Studies of Seismic Steel Beam-to-Column Moment Connections,* M. Eng. Thesis, Dept. of Civil Engineering, University of California, Berkeley, 1995.

[8] Bleich, F., *Buckling Strength of Metal Structures,* McGraw-Hill, New York, 1952.

[9] Broek, D., *Elementary Engineering Fracture Mechanics*, Martinus Nijhoff, The Hague, 1986.

[10] Feder, D. and Lee, G. C., *Residual Stress and the Strength of Members of High Strength Steel,* Fritz Laboratory Report 269.2, Lehigh University, 1959.

[11] Griffith, A. A., "The Phenomena of Rupture and Flow in Solids," *Philosophical Transactions, Royal Society of London,* **A221**, 163-198, 1920.

[12] Hibbitt, Karlsson, and Sorensen, Inc., *ABAQUS Version 5.4.*

[13] Irwin, G. R., "Onset of Fast Crack Propagation in High Strength Steel and Aluminum Alloys," *Sagamore Research Conference Proceedings,* **2**, 289-305, 1956.

[14] Irwin, G. R., "Analysis of Stresses and Strains near the End of a Crack Traversing a Plate," *Journal of Applied Mechanics,* **24**, 361-364, 1957.

[15] Irwin, G. R., "A Summary of Fracture Mechanics Concepts," *Journal of Testing & Evaluation,* **11**, 56-65, 1983.

[16] Kirkaldy, D., *Results of an Experimental Inquiry into the Tensile Strength and Other Properties of Various Kinds of Wrought-Iron and Steel,* 2nd ed., London, Hamilton, Adams & co. 1862.

[17] Ludwik, P. and Scheu, R., "Über Kerbwirkungen bei Flusseisen," *Stahl und Eisen,* 1923.

[18] MacGregor, C. W., "The Yield Point of Mild Steel," *Transactions of the American Society of Mechanical Engineers,* APM-53-15, 187-200, 1931.

[19] Neuber, H., *Kerbspannungslehre,* 2nd ed., Springer-Verlag, Berlin, 1958.

[20] Novak, S. R., "Resistance to Plane-Stress Fracture (R-Curve Behavior) of A572 Structural Steel," *ASTM STP 591,* American Society for Testing and Materials, Philadelphia, 1976.

[21] Peterson, R. E., *Stress Concentration Factors for Design,* Wiley, New York, 1974.

[22] Popov, E. P. and Pinkney, R. B., "Cyclic Yield Reversal in Steel Building Connections," *Journal of Structural Division, ASCE,* **95**, ST3, 327-353, 1969.

[23] Popov, E. P. and Stephen, R. M., "Cyclic Loading of Full Size Steel Connections," *American Iron and Steel Institute, Steel Research for Construction Bulletin No. 21*, 1972.

[24] Rice, J. R., "A Path Independent Integral and the Approximate Analysis of Strain Concentration by Notches and Cracks," *Journal of Applied Mechanics,* **35**, 379-386, June, 1968.

[25] Rolfe, S. T. and Barsom, J. M., *Fracture and Fatigue Control in Structures, Applications of Fracture Mechanics,* 2nd ed., Prentice-Hall, Englewood Cliffs, N.J., 1987.

[26] Roberts, R., Irwin, G. R., Krishna, G. V. and Yen, B. T., "Fracture Toughness of Bridge Steels - Phase II Final Report," *Fritz Engineering Laboratory Report No. 379.2,* Lehigh University, June 1974.

[27] Suresh, S., *Fatigue of Materials,* Cambridge University Press, 1991. (Reprint 1994)

[28] Timoshenko, S., *Strength of Material, Part II, Advanced Theory and Problems,* 3rd ed., D. Van Nostrand Company, Inc., 1956.

[29] Westergaard, H. M., "Bearing Pressures and Cracks," *Journal of Applied Mechanics,* **6**, 49-53, 1939.

[30] Youssef, N. F. G., Bonowitz, D. and Gross, J. L., "A Survey of Steel Moment-Resisting Frame Buildings Affected by the 1994 Northridge Earthquake," *National Institute of Standards and Technology, Report No. NISTIR 5625,* US Department of Commerce, April 1995.

EARTHQUAKE ENGINEERING RESEARCH CENTER REPORT SERIES

EERC reports are available from the National Information Service for Earthquake Engineering (NISEE) and from the National Technical Information Service (NTIS). Numbers in parentheses are Accession Numbers assigned by the National Technical Information Service; these are followed by a price code. Contact NTIS, 5285 Port Royal Road, Springfield Virginia, 22161 for more information. Reports without Accession Numbers were not available from NTIS at the time of printing. For a current complete list of EERC reports (from EERC 67-1) and availablity information, please contact University of California, EERC, NISEE, 1301 South 46th Street, Richmond, California 94804-4698.

UCB/EERC-84/01 "Pseudodynamic Test Method for Seismic Performance Evaluation: Theory and Implementation," by Shing, P.-S.B. and Mahin, S.A., January 1984, (PB84 190 644)A08.

UCB/EERC-84/02 "Dynamic Response Behavior of Kiang Hong Dian Dam," by Clough, R.W., Chang, K.-T., Chen, H.-Q. and Stephen, R.M., April 1984, (PB84 209 402)A08.

UCB/EERC-84/03 "Refined Modelling of Reinforced Concrete Columns for Seismic Analysis," by Kaba, S.A. and Mahin, S.A., April 1984, (PB84 234 384)A06.

UCB/EERC-84/04 "A New Floor Response Spectrum Method for Seismic Analysis of Multiply Supported Secondary Systems," by Asfura, A. and Der Kiureghian, A., June 1984, (PB84 239 417)A06.

UCB/EERC-84/05 "Earthquake Simulation Tests and Associated Studies of a 1/5th-scale Model of a 7-Story R/C Frame-Wall Test Structure," by Bertero, V.V., Aktan, A.E., Charney, F.A. and Sause, R., June 1984, (PB84 239 409)A09.

UCB/EERC-84/06 "Unassigned," by Unassigned, 1984.

UCB/EERC-84/07 "Behavior of Interior and Exterior Flat-Plate Connections Subjected to Inelastic Load Reversals," by Zee, H.L. and Moehle, J.P., August 1984, (PB86 117 629/AS)A07.

UCB/EERC-84/08 "Experimental Study of the Seismic Behavior of a Two-Story Flat-Plate Structure," by Moehle, J.P. and Diebold, J.W., August 1984, (PB86 122 553/AS)A12.

UCB/EERC-84/09 "Phenomenological Modeling of Steel Braces under Cyclic Loading," by Ikeda, K., Mahin, S.A. and Dermitzakis, S.N., May 1984, (PB86 132 198/AS)A08.

UCB/EERC-84/10 "Earthquake Analysis and Response of Concrete Gravity Dams," by Fenves, G.L. and Chopra, A.K., August 1984, (PB85 193 902/AS)A11.

UCB/EERC-84/11 "EAGD-84: A Computer Program for Earthquake Analysis of Concrete Gravity Dams," by Fenves, G.L. and Chopra, A.K., August 1984, (PB85 193 613/AS)A05.

UCB/EERC-84/12 "A Refined Physical Theory Model for Predicting the Seismic Behavior of Braced Steel Frames," by Ikeda, K. and Mahin, S.A., July 1984, (PB85 191 450/AS)A09.

UCB/EERC-84/13 "Earthquake Engineering Research at Berkeley - 1984," by EERC, August 1984, (PB85 197 341/AS)A10.

UCB/EERC-84/14 "Moduli and Damping Factors for Dynamic Analyses of Cohesionless Soils," by Seed, H.B., Wong, R.T., Idriss, I.M. and Tokimatsu, K., September 1984, (PB85 191 468/AS)A04.

UCB/EERC-84/15 "The Influence of SPT Procedures in Soil Liquefaction Resistance Evaluations," by Seed, H.B., Tokimatsu, K., Harder, L.F. and Chung, R.M., October 1984, (PB85 191 732/AS)A04.

UCB/EERC-84/16 "Simplified Procedures for the Evaluation of Settlements in Sands Due to Earthquake Shaking," by Tokimatsu, K. and Seed, H.B., October 1984, (PB85 197 887/AS)A03.

UCB/EERC-84/17 "Evaluation of Energy Absorption Characteristics of Highway Bridges Under Seismic Conditions - Volume I (PB90 262 627)A16 and Volume II (Appendices) (PB90 262 635)A13," by Imbsen, R.A. and Penzien, J., September 1986.

UCB/EERC-84/18 "Structure-Foundation Interactions under Dynamic Loads," by Liu, W.D. and Penzien, J., November 1984, (PB87 124 889/AS)A11.

UCB/EERC-84/19 "Seismic Modelling of Deep Foundations," by Chen, C.-H. and Penzien, J., November 1984, (PB87 124 798/AS)A07.

UCB/EERC-84/20 "Dynamic Response Behavior of Quan Shui Dam," by Clough, R.W., Chang, K.-T., Chen, H.-Q., Stephen, R.M., Ghanaat, Y. and Qi, J.-H., November 1984, (PB86 115177/AS)A07.

UCB/EERC-85/01 "Simplified Methods of Analysis for Earthquake Resistant Design of Buildings," by Cruz, E.F. and Chopra, A.K., February 1985, (PB86 112299/AS)A12.

UCB/EERC-85/02 "Estimation of Seismic Wave Coherency and Rupture Velocity using the SMART 1 Strong-Motion Array Recordings," by Abrahamson, N.A., March 1985, (PB86 214 343)A07.

UCB/EERC-85/03 "Dynamic Properties of a Thirty Story Condominium Tower Building," by Stephen, R.M., Wilson, E.L. and Stander, N., April 1985, (PB86 118965/AS)A06.

UCB/EERC-85/04 "Development of Substructuring Techniques for On-Line Computer Controlled Seismic Performance Testing," by Dermitzakis, S. and Mahin, S., February 1985, (PB86 132941/AS)A08.

UCB/EERC-85/05 "A Simple Model for Reinforcing Bar Anchorages under Cyclic Excitations," by Filippou, F.C., March 1985, (PB86 112 919/AS)A05.

UCB/EERC-85/06 "Racking Behavior of Wood-framed Gypsum Panels under Dynamic Load," by Oliva, M.G., June 1985, (PB90 262 643)A04.

UCB/EERC-85/07 "Earthquake Analysis and Response of Concrete Arch Dams," by Fok, K.-L. and Chopra, A.K., June 1985, (PB86 139672/AS)A10.

UCB/EERC-85/08 "Effect of Inelastic Behavior on the Analysis and Design of Earthquake Resistant Structures," by Lin, J.P. and Mahin, S.A., June 1985, (PB86 135340/AS)A08.

UCB/EERC-85/09 "Earthquake Simulator Testing of a Base-Isolated Bridge Deck," by Kelly, J.M., Buckle, I.G. and Tsai, H.-C., January 1986, (PB87 124 152/AS)A06.

UCB/EERC-85/10 "Simplified Analysis for Earthquake Resistant Design of Concrete Gravity Dams," by Fenves, G.L. and Chopra, A.K., June 1986, (PB87 124 160/AS)A08.

UCB/EERC-85/11 "Dynamic Interaction Effects in Arch Dams," by Clough, R.W., Chang, K.-T., Chen, H.-Q. and Ghanaat, Y., October 1985, (PB86 135027/AS)A05.

UCB/EERC-85/12 "Dynamic Response of Long Valley Dam in the Mammoth Lake Earthquake Series of May 25-27, 1980," by Lai, S. and Seed, H.B., November 1985, (PB86 142304/AS)A05.

UCB/EERC-85/13 "A Methodology for Computer-Aided Design of Earthquake-Resistant Steel Structures," by Austin, M.A., Pister, K.S. and Mahin, S.A., December 1985, (PB86 159480/AS)A10 .

UCB/EERC-85/14 "Response of Tension-Leg Platforms to Vertical Seismic Excitations," by Liou, G.-S., Penzien, J. and Yeung, R.W., December 1985, (PB87 124 871/AS)A08.

UCB/EERC-85/15 "Cyclic Loading Tests of Masonry Single Piers: Volume 4 - Additional Tests with Height to Width Ratio of 1," by Sveinsson, B., McNiven, H.D. and Sucuoglu, H., December 1985, (PB87 165031/AS)A08.

UCB/EERC-85/16 "An Experimental Program for Studying the Dynamic Response of a Steel Frame with a Variety of Infill Partitions," by Yanev, B. and McNiven, H.D., December 1985, (PB90 262 676)A05.

UCB/EERC-86/01 "A Study of Seismically Resistant Eccentrically Braced Steel Frame Systems," by Kasai, K. and Popov, E.P., January 1986, (PB87 124 178/AS)A14.

UCB/EERC-86/02 "Design Problems in Soil Liquefaction," by Seed, H.B., February 1986, (PB87 124 186/AS)A03.

UCB/EERC-86/03 "Implications of Recent Earthquakes and Research on Earthquake-Resistant Design and Construction of Buildings," by Bertero, V.V., March 1986, (PB87 124 194/AS)A05.

UCB/EERC-86/04 "The Use of Load Dependent Vectors for Dynamic and Earthquake Analyses," by Leger, P., Wilson, E.L. and Clough, R.W., March 1986, (PB87 124 202/AS)A12.

UCB/EERC-86/05 "Two Beam-To-Column Web Connections," by Tsai, K.-C. and Popov, E.P., April 1986, (PB87 124 301/AS)A04.

UCB/EERC-86/06 "Determination of Penetration Resistance for Coarse-Grained Soils using the Becker Hammer Drill," by Harder, L.F. and Seed, H.B., May 1986, (PB87 124 210/AS)A07.

UCB/EERC-86/07 "A Mathematical Model for Predicting the Nonlinear Response of Unreinforced Masonry Walls to In-Plane Earthquake Excitations," by Mengi, Y. and McNiven, H.D., May 1986, (PB87 124 780/AS)A06.

UCB/EERC-86/08 "The 19 September 1985 Mexico Earthquake: Building Behavior," by Bertero, V.V., July 1986.

UCB/EERC-86/09 "EACD-3D: A Computer Program for Three-Dimensional Earthquake Analysis of Concrete Dams," by Fok, K.-L., Hall, J.F. and Chopra, A.K., July 1986, (PB87 124 228/AS)A08.

UCB/EERC-86/10 "Earthquake Simulation Tests and Associated Studies of a 0.3-Scale Model of a Six-Story Concentrically Braced Steel Structure," by Uang, C.-M. and Bertero, V.V., December 1986, (PB87 163 564/AS)A17.

UCB/EERC-86/11 "Mechanical Characteristics of Base Isolation Bearings for a Bridge Deck Model Test," by Kelly, J.M., Buckle, I.G. and Koh, C.-G., November 1987, (PB90 262 668)A04.

UCB/EERC-86/12 "Effects of Axial Load on Elastomeric Isolation Bearings," by Koh, C.-G. and Kelly, J.M., November 1987, PB88-179015(A06).

UCB/EERC-87/01 "The FPS Earthquake Resisting System: Experimental Report," by Zayas, V.A., Low, S.S. and Mahin, S.A., June 1987, (PB88 170 287)A06.

UCB/EERC-87/02 "Earthquake Simulator Tests and Associated Studies of a 0.3-Scale Model of a Six-Story Eccentrically Braced Steel Structure," by Whittaker, A., Uang, C.-M. and Bertero, V.V., July 1987, (PB88 166 707/AS)A18.

UCB/EERC-87/03 "A Displacement Control and Uplift Restraint Device for Base-Isolated Structures," by Kelly, J.M., Griffith, M.C. and Aiken, I.D., April 1987, (PB88 169 933)A04.

UCB/EERC-87/04 "Earthquake Simulator Testing of a Combined Sliding Bearing and Rubber Bearing Isolation System," by Kelly, J.M. and Chalhoub, M.S., December 1990, PB92-192962(A09).

UCB/EERC-87/05 "Three-Dimensional Inelastic Analysis of Reinforced Concrete Frame-Wall Structures," by Moazzami, S. and Bertero, V.V., May 1987, (PB88 169 586/AS)A08.

UCB/EERC-87/06 "Experiments on Eccentrically Braced Frames with Composite Floors," by Ricles, J. and Popov, E., June 1987, (PB88 173 067/AS)A14.

UCB/EERC-87/07 "Dynamic Analysis of Seismically Resistant Eccentrically Braced Frames," by Ricles, J. and Popov, E., June 1987, (PB88 173 075/AS)A16.

UCB/EERC-87/08 "Undrained Cyclic Triaxial Testing of Gravels-The Effect of Membrane Compliance," by Evans, M.D. and Seed, H.B., July 1987, (PB88 173 257)A19.

UCB/EERC-87/09 "Hybrid Solution Techniques for Generalized Pseudo-Dynamic Testing," by Thewalt, C. and Mahin, S.A., July 1987, (PB 88 179 007)A07.

UCB/EERC-87/10 "Ultimate Behavior of Butt Welded Splices in Heavy Rolled Steel Sections," by Bruneau, M., Mahin, S.A. and Popov, E.P., September 1987, (PB90 254 285)A07.

UCB/EERC-87/11 "Residual Strength of Sand from Dam Failures in the Chilean Earthquake of March 3, 1985," by De Alba, P., Seed, H.B., Retamal, E. and Seed, R.B., September 1987, (PB88 174 321/AS)A03.

UCB/EERC-87/12 "Inelastic Seismic Response of Structures with Mass or Stiffness Eccentricities in Plan," by Bruneau, M. and Mahin, S.A., September 1987, (PB90 262 650/AS)A14.

UCB/EERC-87/13 "CSTRUCT: An Interactive Computer Environment for the Design and Analysis of Earthquake Resistant Steel Structures," by Austin, M.A., Mahin, S.A. and Pister, K.S., September 1987, (PB88 173 339/AS)A06.

UCB/EERC-87/14 "Experimental Study of Reinforced Concrete Columns Subjected to Multi-Axial Loading," by Low, S.S. and Moehle, J.P., September 1987, (PB88 174 347/AS)A07.

UCB/EERC-87/15 "Relationships between Soil Conditions and Earthquake Ground Motions in Mexico City in the Earthquake of Sept. 19, 1985," by Seed, H.B., Romo, M.P., Sun, J., Jaime, A. and Lysmer, J., October 1987, (PB88 178 991)A06.

UCB/EERC-87/16 "Experimental Study of Seismic Response of R. C. Setback Buildings," by Shahrooz, B.M. and Moehle, J.P., October 1987, (PB88 176 359)A16.

UCB/EERC-87/17 "The Effect of Slabs on the Flexural Behavior of Beams," by Pantazopoulou, S.J. and Moehle, J.P., October 1987, (PB90 262 700)A07.

UCB/EERC-87/18 "Design Procedure for R-FBI Bearings," by Mostaghel, N. and Kelly, J.M., November 1987, (PB90 262 718)A04.

UCB/EERC-87/19 "Analytical Models for Predicting the Lateral Response of R C Shear Walls: Evaluation of their Reliability," by Vulcano, A. and Bertero, V.V., November 1987, (PB88 178 983)A05.

UCB/EERC-87/20 "Earthquake Response of Torsionally-Coupled Buildings," by Hejal, R. and Chopra, A.K., December 1987, PB90-208638(A15).

UCB/EERC-87/21 "Dynamic Reservoir Interaction with Monticello Dam," by Clough, R.W., Ghanaat, Y. and Qiu, X-F., December 1987, (PB88 179 023)A07.

UCB/EERC-87/22 "Strength Evaluation of Coarse-Grained Soils," by Siddiqi, F.H., Seed, R.B., Chan, C.K., Seed, H.B. and Pyke, R.M., December 1987, (PB88 179 031)A04.

UCB/EERC-88/01 "Seismic Behavior of Concentrically Braced Steel Frames," by Khatib, I., Mahin, S.A. and Pister, K.S., January 1988, (PB91 210 898/AS)A11.

UCB/EERC-88/02 "Experimental Evaluation of Seismic Isolation of Medium-Rise Structures Subject to Uplift," by Griffith, M.C., Kelly, J.M., Coveney, V.A. and Koh, C.G., January 1988, (PB91 217 950/AS)A09.

UCB/EERC-88/03 "Cyclic Behavior of Steel Double Angle Connections," by Astaneh-Asl, A. and Nader, M.N., January 1988, (PB91 210 872)A05.

UCB/EERC-88/04 "Re-evaluation of the Slide in the Lower San Fernando Dam in the Earthquake of Feb. 9, 1971," by Seed, H.B., Seed, R.B., Harder, L.F. and Jong, H.-L., April 1988, (PB91 212 456/AS)A07.

UCB/EERC-88/05 "Experimental Evaluation of Seismic Isolation of a Nine-Story Braced Steel Frame Subject to Uplift," by Griffith, M.C., Kelly, J.M. and Aiken, I.D., May 1988, (PB91 217 968/AS)A07.

UCB/EERC-88/06 "DRAIN-2DX User Guide.," by Allahabadi, R. and Powell, G.H., March 1988, (PB91 212 530)A12.

UCB/EERC-88/07 "Theoretical and Experimental Studies of Cylindrical Water Tanks in Base-Isolated Structures," by Chalhoub, M.S. and Kelly, J.M., April 1988, (PB91 217 976/AS)A05.

UCB/EERC-88/08 "Analysis of Near-Source Waves: Separation of Wave Types Using Strong Motion Array Recording," by Darragh, R.B., June 1988, (PB91 212 621)A08.

UCB/EERC-88/09 "Alternatives to Standard Mode Superposition for Analysis of Non-Classically Damped Systems," by Kusainov, A.A. and Clough, R.W., June 1988, (PB91 217 992/AS)A04.

UCB/EERC-88/10 "The Landslide at the Port of Nice on October 16, 1979," by Seed, H.B., Seed, R.B., Schlosser, F., Blondeau, F. and Juran, I., June 1988, (PB91 210 914)A05.

UCB/EERC-88/11 "Liquefaction Potential of Sand Deposits Under Low Levels of Excitation," by Carter, D.P. and Seed, H.B., August 1988, (PB91 210 880)A15.

UCB/EERC-88/12 "Nonlinear Analysis of Reinforced Concrete Frames Under Cyclic Load Reversals," by Filippou, F.C. and Issa, A., September 1988, (PB91 212 589)A07.

UCB/EERC-88/13 "Implications of Recorded Earthquake Ground Motions on Seismic Design of Building Structures," by Uang, C.-M. and Bertero, V.V., November 1988, (PB91 212 548)A06.

UCB/EERC-88/14 "An Experimental Study of the Behavior of Dual Steel Systems," by Whittaker, A.S. , Uang, C.-M. and Bertero, V.V., September 1988, (PB91 212 712)A16.

UCB/EERC-88/15 "Dynamic Moduli and Damping Ratios for Cohesive Soils," by Sun, J.I., Golesorkhi, R. and Seed, H.B., August 1988, (PB91 210 922)A04.

UCB/EERC-88/16 "Reinforced Concrete Flat Plates Under Lateral Load: An Experimental Study Including Biaxial Effects," by Pan, A. and Moehle, J.P., October 1988, (PB91 210 856)A13.

UCB/EERC-88/17 "Earthquake Engineering Research at Berkeley - 1988," by EERC, November 1988, (PB91 210 864)A10.

UCB/EERC-88/18 "Use of Energy as a Design Criterion in Earthquake-Resistant Design," by Uang, C.-M. and Bertero, V.V., November 1988, (PB91 210 906/AS)A04.

UCB/EERC-88/19 "Steel Beam-Column Joints in Seismic Moment Resisting Frames," by Tsai, K.-C. and Popov, E.P., November 1988, (PB91 217 984/AS)A20.

UCB/EERC-88/20 "Base Isolation in Japan, 1988," by Kelly, J.M., December 1988, (PB91 212 449)A05.

UCB/EERC-89/01 "Behavior of Long Links in Eccentrically Braced Frames," by Engelhardt, M.D. and Popov, E.P., January 1989, (PB92 143 056)A18.

UCB/EERC-89/02 "Earthquake Simulator Testing of Steel Plate Added Damping and Stiffness Elements," by Whittaker, A., Bertero, V.V., Alonso, J. and Thompson, C., January 1989, (PB91 229 252/AS)A10.

UCB/EERC-89/03 "Implications of Site Effects in the Mexico City Earthquake of Sept. 19, 1985 for Earthquake-Resistant Design Criteria in the San Francisco Bay Area of California," by Seed, H.B. and Sun, J.I., March 1989, (PB91 229 369/AS)A07.

UCB/EERC-89/04 "Earthquake Analysis and Response of Intake-Outlet Towers," by Goyal, A. and Chopra, A.K., July 1989, (PB91 229 286/AS)A19.

UCB/EERC-89/05 "The 1985 Chile Earthquake: An Evaluation of Structural Requirements for Bearing Wall Buildings," by Wallace, J.W. and Moehle, J.P., July 1989, (PB91 218 008/AS)A13.

UCB/EERC-89/06 "Effects of Spatial Variation of Ground Motions on Large Multiply-Supported Structures," by Hao, H., July 1989, (PB91 229 161/AS)A08.

UCB/EERC-89/07 "EADAP - Enhanced Arch Dam Analysis Program: Users's Manual," by Ghanaat, Y. and Clough, R.W., August 1989, (PB91 212 522)A06.

UCB/EERC-89/08 "Seismic Performance of Steel Moment Frames Plastically Designed by Least Squares Stress Fields," by Ohi, K. and Mahin, S.A., August 1989, (PB91 212 597)A05.

UCB/EERC-89/09 "Feasibility and Performance Studies on Improving the Earthquake Resistance of New and Existing Buildings Using the Friction Pendulum System," by Zayas, V., Low, S., Mahin, S.A. and Bozzo, L., July 1989, (PB92 143 064)A14.

UCB/EERC-89/10 "Measurement and Elimination of Membrane Compliance Effects in Undrained Triaxial Testing," by Nicholson, P.G., Seed, R.B. and Anwar, H., September 1989, (PB92 139 641/AS)A13.

UCB/EERC-89/11 "Static Tilt Behavior of Unanchored Cylindrical Tanks," by Lau, D.T. and Clough, R.W., September 1989, (PB92 143 049)A10.

UCB/EERC-89/12 "ADAP-88: A Computer Program for Nonlinear Earthquake Analysis of Concrete Arch Dams," by Fenves, G.L., Mojtahedi, S. and Reimer, R.B., September 1989, (PB92 139 674/AS)A07.

UCB/EERC-89/13 "Mechanics of Low Shape Factor Elastomeric Seismic Isolation Bearings," by Aiken, I.D., Kelly, J.M. and Tajirian, F.F., November 1989, (PB92 139 732/AS)A09.

UCB/EERC-89/14 "Preliminary Report on the Seismological and Engineering Aspects of the October 17, 1989 Santa Cruz (Loma Prieta) Earthquake," by EERC, October 1989, (PB92 139 682/AS)A04.

UCB/EERC-89/15 "Experimental Studies of a Single Story Steel Structure Tested with Fixed, Semi-Rigid and Flexible Connections," by Nader, M.N. and Astaneh-Asl, A., August 1989, (PB91 229 211/AS)A10.

UCB/EERC-89/16 "Collapse of the Cypress Street Viaduct as a Result of the Loma Prieta Earthquake," by Nims, D.K., Miranda, E., Aiken, I.D., Whittaker, A.S. and Bertero, V.V., November 1989, (PB91 217 935/AS)A05.

UCB/EERC-90/01 "Mechanics of High-Shape Factor Elastomeric Seismic Isolation Bearings," by Kelly, J.M., Aiken, I.D. and Tajirian, F.F., March 1990.

UCB/EERC-90/02 "Javid's Paradox: The Influence of Preform on the Modes of Vibrating Beams," by Kelly, J.M., Sackman, J.L. and Javid, A., May 1990, (PB91 217 943/AS)A03.

UCB/EERC-90/03 "Earthquake Simulator Testing and Analytical Studies of Two Energy-Absorbing Systems for Multistory Structures," by Aiken, I.D. and Kelly, J.M., October 1990, (PB92 192 988)A13.

UCB/EERC-90/04 "Unassigned," by Unassigned, 1990.

UCB/EERC-90/05 "Preliminary Report on the Principal Geotechnical Aspects of the October 17, 1989 Loma Prieta Earthquake," by Seed, R.B., Dickenson, S.E., Riemer, M.F., Bray, J.D., Sitar, N., Mitchell, J.K., Idriss, I.M., Kayen, R.E., Kropp, A., Harder, L.F., Jr. and Power, M.S., April 1990, (PB 192 970)A08.

UCB/EERC-90/06 "Models of Critical Regions in Reinforced Concrete Frames Under Seismic Excitations," by Zulfiqar, N. and Filippou, F.C., May 1990.

UCB/EERC-90/07 "A Unified Earthquake-Resistant Design Method for Steel Frames Using ARMA Models," by Takewaki, I., Conte, J.P., Mahin, S.A. and Pister, K.S., June 1990, PB92-192947(A06).

UCB/EERC-90/08 "Soil Conditions and Earthquake Hazard Mitigation in the Marina District of San Francisco," by Mitchell, J.K., Masood, T., Kayen, R.E. and Seed, R.B., May 1990, (PB 193 267/AS)A04.

UCB/EERC-90/09 "Influence of the Earthquake Ground Motion Process and Structural Properties on Response Characteristics of Simple Structures," by Conte, J.P., Pister, K.S. and Mahin, S.A., July 1990, (PB92 143 064)A15.

UCB/EERC-90/10 "Experimental Testing of the Resilient-Friction Base Isolation System," by Clark, P.W. and Kelly, J.M., July 1990, (PB92 143 072)A08.

UCB/EERC-90/11 "Seismic Hazard Analysis: Improved Models, Uncertainties and Sensitivities," by Araya, R. and Der Kiureghian, A., March 1988, PB92-193010(A08).

UCB/EERC-90/12 "Effects of Torsion on the Linear and Nonlinear Seismic Response of Structures," by Sedarat, H. and Bertero, V.V., September 1989, (PB92 193 002/AS)A15.

UCB/EERC-90/13 "The Effects of Tectonic Movements on Stresses and Deformations in Earth Embankments," by Bray, J. D., Seed, R. B. and Seed, H. B., September 1989, PB92-192996(A18).

UCB/EERC-90/14 "Inelastic Seismic Response of One-Story, Asymmetric-Plan Systems," by Goel, R.K. and Chopra, A.K., October 1990, (PB93 114 767)A11.

UCB/EERC-90/15 "Dynamic Crack Propagation: A Model for Near-Field Ground Motion.," by Seyyedian, H. and Kelly, J.M., 1990.

UCB/EERC-90/16 "Sensitivity of Long-Period Response Spectra to System Initial Conditions," by Blasquez, R., Ventura, C. and Kelly, J.M., 1990.

UCB/EERC-90/17 "Behavior of Peak Values and Spectral Ordinates of Near-Source Strong Ground-Motion over a Dense Array," by Niazi, M., June 1990, (PB93 114 833)A07.

UCB/EERC-90/18 "Material Characterization of Elastomers used in Earthquake Base Isolation," by Papoulia, K.D. and Kelly, J.M., 1990, PB94-190063(A08).

UCB/EERC-90/19 "Cyclic Behavior of Steel Top-and-Bottom Plate Moment Connections," by Harriott, J.D. and Astaneh-Asl, A., August 1990, (PB91 229 260/AS)A05.

UCB/EERC-90/20 "Seismic Response Evaluation of an Instrumented Six Story Steel Building," by Shen, J.-H. and Astaneh-Asl, A., December 1990, (PB91 229 294/AS)A04.

UCB/EERC-90/21 "Observations and Implications of Tests on the Cypress Street Viaduct Test Structure," by Bollo, M., Mahin, S.A., Moehle, J.P., Stephen, R.M. and Qi, X., December 1990, (PB93 114 775)A13.

UCB/EERC-91/01 "Experimental Evaluation of Nitinol for Energy Dissipation in Structures," by Nims, D.K., Sasaki, K.K. and Kelly, J.M., 1991.

UCB/EERC-91/02 "Displacement Design Approach for Reinforced Concrete Structures Subjected to Earthquakes," by Qi, X. and Moehle, J.P., January 1991, (PB93 114 569/AS)A09.

UCB/EERC-91/03 "A Long-Period Isolation System Using Low-Modulus High-Damping Isolators for Nuclear Facilities at Soft-Soil Sites," by Kelly, J.M., March 1991, (PB93 114 577/AS)A10.

UCB/EERC-91/04 "Dynamic and Failure Characteristics of Bridgestone Isolation Bearings," by Kelly, J.M., April 1991, (PB93 114 528)A05.

UCB/EERC-91/05 "Base Sliding Response of Concrete Gravity Dams to Earthquakes," by Chopra, A.K. and Zhang, L., May 1991, (PB93 114 544/AS)A05.

UCB/EERC-91/06 "Computation of Spatially Varying Ground Motion and Foundation-Rock Impedance Matrices for Seismic Analysis of Arch Dams," by Zhang, L. and Chopra, A.K., May 1991, (PB93 114 825)A07.

UCB/EERC-91/07 "Estimation of Seismic Source Processes Using Strong Motion Array Data," by Chiou, S.-J., July 1991, (PB93 114 551/AS)A08.

UCB/EERC-91/08 "A Response Spectrum Method for Multiple-Support Seismic Excitations," by Der Kiureghian, A. and Neuenhofer, A., August 1991, (PB93 114 536)A04.

UCB/EERC-91/09 "A Preliminary Study on Energy Dissipating Cladding-to-Frame Connection," by Cohen, J.M. and Powell, G.H., September 1991, (PB93 114 510)A05.

UCB/EERC-91/10 "Evaluation of Seismic Performance of a Ten-Story RC Building During the Whittier Narrows Earthquake," by Miranda, E. and Bertero, V.V., October 1991, (PB93 114 783)A06.

UCB/EERC-91/11 "Seismic Performance of an Instrumented Six-Story Steel Building," by Anderson, J.C. and Bertero, V.V., November 1991, (PB93 114 809)A07.

UCB/EERC-91/12 "Performance of Improved Ground During the Loma Prieta Earthquake," by Mitchell, J.K. and Wentz, Jr., F.J., October 1991, (PB93 114 791)A06.

UCB/EERC-91/13 "Shaking Table - Structure Interaction," by Rinawi, A.M. and Clough, R.W., October 1991, (PB93 114 917)A13.

UCB/EERC-91/14 "Cyclic Response of RC Beam-Column Knee Joints: Test and Retrofit," by Mazzoni, S., Moehle, J.P. and Thewalt, C.R., October 1991, (PB93 120 277)A03.

UCB/EERC-91/15 "Design Guidelines for Ductility and Drift Limits: Review of State-of-the-Practice and State-of-the-Art in Ductility and Drift-Based Earthquake-Resistant Design of Buildings," by Bertero, V.V., Anderson, J.C., Krawinkler, H., Miranda, E. and The CUREe and The Kajima Research Teams, July 1991, (PB93 120 269)A08.

UCB/EERC-91/16 "Evaluation of the Seismic Performance of a Thirty-Story RC Building," by Anderson, J.C., Miranda, E., Bertero, V.V. and The Kajima Project Research Team, July 1991, (PB93 114 841)A12.

UCB/EERC-91/17 "A Fiber Beam-Column Element for Seismic Response Analysis of Reinforced Concrete Structures," by Taucer, F., Spacone, E. and Filippou, F.C., December 1991, (PB94 117 629AS)A07.

UCB/EERC-91/18 "Investigation of the Seismic Response of a Lightly-Damped Torsionally-Coupled Building," by Boroschek, R. and Mahin, S.A., December 1991, (PB93 120 335)A13.

UCB/EERC-92/01 "Studies of a 49-Story Instrumented Steel Structure Shaken During the Loma Prieta Earthquake," by Chen, C.-C., Bonowitz, D. and Astaneh-Asl, A., February 1992, (PB93 221 778)A08.

UCB/EERC-92/02 "Response of the Dumbarton Bridge in the Loma Prieta Earthquake," by Fenves, G.L., Filippou, F.C. and Sze, D.T., January 1992, (PB93 120 319)A09.

UCB/EERC-92/03 "Models for Nonlinear Earthquake Analysis of Brick Masonry Buildings," by Mengi, Y., McNiven, H.D. and Tanrikulu, A.K., March 1992, (PB93 120 293)A08.

UCB/EERC-92/04 "Shear Strength and Deformability of RC Bridge Columns Subjected to Inelastic Cyclic Displacements," by Aschheim, M. and Moehle, J.P., March 1992, (PB93 120 327)A06.

UCB/EERC-92/05 "Parameter Study of Joint Opening Effects on Earthquake Response of Arch Dams," by Fenves, G.L., Mojtahedi, S. and Reimer, R.B., April 1992, (PB93 120 301)A04.

UCB/EERC-92/06 "Seismic Behavior and Design of Semi-Rigid Steel Frames," by Nader, M.N. and Astaneh-Asl, A., May 1992, PB93-221760(A17).

UCB/EERC-92/07 "A Beam Element for Seismic Damage Analysis," by Spacone, E., Ciampi, V. and Filippou, F.C., August 1992, (PB95-192126)A06.

UCB/EERC-92/08 "Nonlinear Static and Dynamic Analysis of Reinforced Concrete Subassemblages," by Filippou, F.C., D'Ambrisi, A. and Issa, A., August 1992, PB95-192175(A09).

UCB/EERC-92/09 "Evaluation of Code Accidental-Torsion Provisions Using Earthquake Records from Three Nominally Symmetric-Plan Buildings," by De la Llera, J.C. and Chopra, A.K., September 1992, (PB94 117 611)A08.

UCB/EERC-92/10 "Slotted Bolted Connection Energy Dissipators," by Grigorian, C.E., Yang, T.-S. and Popov, E.P., July 1992, (PB92 120 285)A03.

UCB/EERC-92/11 "Mechanical Characteristics of Neoprene Isolation Bearings," by Kelly, J.M. and Quiroz, E., August 1992, (PB93 221 729)A07.

UCB/EERC-92/12 "Application of a Mass Damping System to Bridge Structures," by Hasegawa, K. and Kelly, J.M., August 1992, (PB93 221 786)A06.

UCB/EERC-92/13 "Earthquake Engineering Research at Berkeley - 1992," by EERC, October 1992, PB93-223709(A10).

UCB/EERC-92/14 "Earthquake Risk and Insurance," by Brillinger, D.R., October 1992, (PB93 223 352)A03.

UCB/EERC-92/15 "A Friction Mass Damper for Vibration Control," by Inaudi, J.A. and Kelly, J.M., October 1992, (PB93 221 745)A04.

UCB/EERC-92/16 "Tall Reinforced Concrete Buildings: Conceptual Earthquake-Resistant Design Methology," by Bertero, R.D. and Bertero, V.V., December 1992, (PB93 221 695)A12.

UCB/EERC-92/17 "Performance of Tall Buildings During the 1985 Mexico Earthquakes," by Terán-Gilmore, A. and Bertero, V.V., December 1992, (PB93 221 737)A11.

UCB/EERC-92/18 "Dynamic Analysis of Nonlinear Structures using State-Space Formulation and Partitioned Integration Schemes," by Inaudi, J.A. and De la Llera, J.C., December 1992, (PB94 117 702/AS/A05.

UCB/EERC-93/01 "Seismic Performance of an Instrumented Six-Story Reinforced-Concrete Building," by Anderson, J.C. and Bertero, V.V., 1993.

UCB/EERC-93/02 "Evaluation of an Active Variable-Damping-Structure," by Polak, E., Meeker, G., Yamada, K. and Kurata, N., 1993, (PB93 221 711)A05.

UCB/EERC-93/03 "An Experimental Study of Flat-Plate Structures under Vertical and Lateral Loads," by Hwang, S.-H. and Moehle, J.P., February 1993, (PB94 157 690/AS)A13.

UCB/EERC-93/04 "Seismic Performance of a 30-Story Building Located on Soft Soil and Designed According to UBC 1991," by Terán-Gilmore, A. and Bertero, V.V., 1993, (PB93 221 703)A17.

UCB/EERC-93/05 "Multiple-Support Response Spectrum Analysis of the Golden Gate Bridge," by Nakamura, Y., Der Kiureghian, A. and Liu, D., May 1993, (PB93 221 752)A05.

UCB/EERC-93/06 "On the Analysis of Structures with Viscoelastic Dampers," by Inaudi, J.A., Zambrano, A. and Kelly, J.M., August 1993, PB94-165867(A06).

UCB/EERC-93/07 "Earthquake Analysis and Response of Concrete Gravity Dams Including Base Sliding," by Chávez, J.W. and Fenves, G.L., December 1993, (PB94 157 658/AS)A10.

UCB/EERC-93/08 "Model for Anchored Reinforcing Bars under Seismic Excitations," by Monti, G., Spacone, E. and Filippou, F.C., December 1993, PB95-192183(A05).

UCB/EERC-93/09 "A Methodology for Design of Viscoelastic Dampers in Earthquake-Resistant Structures," by Abbas, H. and Kelly, J.M., November 1993, PB94-190071(A10).

UCB/EERC-93/10 "Tuned Mass Dampers Using Viscoelastic Dampers," by Inaudi, J.A., Lopez-Almansa, F. and Kelly, J.M., December 1993.

UCB/EERC-93/11 "Nonlinear Homogeneous Dynamical Systems," by Inaudi, J.A. and Kelly, J.M., December 1993.

UCB/EERC-93/12 "Synthesized Strong Ground Motions for the Seismic Condition Assessment of the Eastern Portion of the San Francisco Bay Bridge," by Bolt, B.A. and Gregor, N.J., December 1993, PB94-165842(A10).

UCB/EERC-93/13 "On the Analysis of Structures with Energy Dissipating Restraints," by Inaudi, J.A., Nims, D.K. and Kelly, J.M., December 1993, PB94-203619(A07).

UCB/EERC-94/01 "Preliminary Report on the Seismological and Engineering Aspects of the January 17, 1994 Northridge Earthquake," by EERC, January 1994, (PB94 157 666/AS)A05.

UCB/EERC-94/02 "Energy Dissipation with Slotted Bolted Connections," by Grigorian, C.E. and Popov, E.P., February 1994, PB94-164605.

UCB/EERC-94/03 "The Influence of Plate Flexibility on the Buckling Load of Elastomeric Isolators," by Kelly, J.M., March 1994, PB95-192134(A04).

UCB/EERC-94/04 "Insitu Test Results from Four Loma Prieta Earthquake Liquefaction Sites: SPT, CPT, DMT and Shear Wave Velocity," by Mitchell, J.K., Lodge, A.L., Coutinho, R.Q., Kayen, R.E., Seed, R.B., Nishio, S. and Stokoe II, K.H., April 1994, PB94-190089(A09).

UCB/EERC-94/05 "Seismic Response of Steep Natural Slopes," by Sitar, N. and Ashford, S.A., May 1994, PB94-203643(A10).

UCB/EERC-94/06 "Small-Scale Testing of a Self-Centering Friction Energy Dissipator for Structures," by Nims, D.K. and Kelly, J.M., August 1994.

UCB/EERC-94/07 "Accidental and Natural Torsion in Earthquake Response and Design of Buildings," by De la Llera, J.C. and Chopra, A.K., June 1994, PB94-203627(A14).

UCB/EERC-94/08 "Preliminary Report on the Principal Geotechnical Aspects of the January 17, 1994 Northridge Earthquake," by Stewart, J.P., Bray, J.D., Seed, R.B. and Sitar, N., June 1994, PB94203635(A12).

UCB/EERC-94/09 "Performance of Steel Building Structures During the Northridge Earthquake," by Bertero, V.V., Anderson, J.C. and Krawinkler, H., August 1994, PB95-112025(A10).

UCB/EERC-94/10 "Manual for Menshin Design of Highway Bridges: Ministry of Construction, Japan," by Sugita, H. and Mahin, S., August 1994, PB95-192100(A08).

UCB/EERC-94/11 "Earthquake Analysis and Response of Two-Level Viaducts," by Singh, S.P. and Fenves, G.L., October 1994, (A09).

UCB/EERC-94/12 "Response of the Northwest Connector in the Landers and Big Bear Earthquakes," by Fenves, G.L. and Desroches, R., December 1994, PB95-192001(A08).

UCB/EERC-95/01 "Geotechnical Reconnaissance of the Effects of the January 17, 1995, Hyogoken-Nanbu Earthquake, Japan," August 1995.

UCB/EERC-95/02 "The Attenuation of Strong Ground Motion Displacement," by Gregor, N.J., June 1995.

UCB/EERC-95/03 "Upgrading Bridge Outrigger Knee Joint Systems," by Stojadinovic, B. and Thewalt, C.R., June 1995.

UCB/EERC-95/04 "Earthquake Hazard Reduction in Historical Buildings Using Seismic Isolation," by Garevski, M., June 1995.

UCB/EERC-95/05 "Final Report on the International Workshop on the Use of Rubber-Based Bearings for the Earthquake Protection of Building," by Kelly, J.M., May 1995.

UCB/EERC-95/06 "Seismic Rehabilitation of Framed Buildings Infilled with Unreinforced Masonry Walls Using Post-Tensioned Steel Braces," by Terán-Gilmore, A., Bertero, V.V. and Youssef, N., June 1995.

UCB/EERC-95/07 "Earthquake Analysis and Resposne of Concrete Arch Dams," by Tan, H. and Chopra, A.K., August 1995.

UCB/EERC-95/08 "Behavior of Pre-Northridge Moment Resisting Steel Connections," by Yang, T.-S. and Popov, E.P., August 1995.